Variability of polycyclic aromatic hydrocarbons and their oxidative derivatives in wintertime Beijing, China.

Atallah. El zein[1], Rachel E. Dunmore[1], Martyn W. Ward[1], Jacqueline F. Hamilton[1], Alastair C. Lewis[2]

[1]Wolfson Atmospheric Chemistry Laboratories, Department of Chemistry, University of York, York, YO10 5DD, United Kingdom
[2]National Centre for Atmospheric Science, University of York, York, YO10 5DD, United Kingdom

Correspondence to: Atallah. El zein (atallah.elzein@york.ac.uk); Alastair C. Lewis (ally.lewis@ncas.ac.uk)

Abstract. Ambient particulate matter (PM) can contain a mix of different toxic species derived from a wide variety of sources. This study quantifies the diurnal variation and nocturnal abundance of 16 Polycyclic Aromatic Hydrocarbons (PAHs), 10 Oxygenated PAHs (OPAHs) and 9 Nitrated PAHs (NPAHs) in ambient PM in central Beijing during winter. Target compounds were identified and quantified using Gas Chromatography – time of flight mass spectrometry (GC-Q-TOF-MS). The total concentration of PAHs varied between 18 and 297 ng m^{-3} over 3 h daytime filter samples and from 23 to 165 ng m^{-3} in 15 h night-time samples. The total concentrations of PAHs over 24 h varied between 37 and 180 ng m^{-3} (mean: 97 ± 43 ng m^{-3}). The total daytime concentrations during high particulate loading conditions for PAHs, OPAHs and NPAHs were 224, 54, and 2.3 ng m^{-3}, respectively. The most abundant PAHs were fluoranthene (33 ng m^{-3}), chrysene (27 ng m^{-3}), pyrene (27 ng m^{-3}), benzo[a]pyrene (27 ng m^{-3}), benzo[b]fluoranthene (25 ng m^{-3}), benzo[a]anthracene (20 ng m^{-3}) and phenanthrene (18 ng m^{-3}). The most abundant OPAHs were 9,10-Anthraquinone (18 ng m^{-3}), 1,8 Naphthalic anhydride (14 ng m^{-3}) and 9-Fluorenone (12 ng m^{-3}) and the three most abundant NPAHs were 9-Nitroanthracene (0.84 ng m^{-3}), 3-Nitrofluoranthene (0.78 ng m^{-3}) and 3-Nitrodibenzofuran (0.45 ng m^{-3}). ∑PAHs and ∑OPAHs showed a strong positive correlation with the gas phase abundance of NO, CO, SO$_2$, and HONO indicating that PAHs and OPAHs can be associated with both local and regional emissions. Diagnostic ratios suggested emissions from traffic road and coal combustion were the predominant sources for PAHs in Beijing, and also revealed the main source of NPAHs to be secondary photochemical formation rather than primary emissions. PM$_{2.5}$ and NPAHs showed a strong correlation with gas phase HONO. 9-Nitroanthracene appeared to undergo a photo-degradation during the daytime and showed a strong positive correlation with ambient HONO (R=0.90, P<0.001). The lifetime excess lung cancer risk for those species that have available toxicological data (16 PAHs, 1 OPAH and 6 NPAHs) was calculated to be in the range 10^{-5} to 10^{-3} (risk per million people range from 26 to 2053).

1 Introduction

Outdoor air pollution contains a complex set of toxicological hazards and has become the largest detrimental environmental effect on human health (WHO/IARC., 2016). Exposure to outdoor high particulate loading of PM$_{2.5}$ (aerodynamic diameter less than 2.5 μm) is linked to harmful health effects, particularly affecting urban populations (Raaschou et al., 2013; Hamra et al., 2014). The major sources of PM$_{2.5}$ in urban areas are

1

incomplete combustion or gas-to-particle conversion, and they contain a varied mix of chemicals including inorganic ions, organic carbon and elemental carbon (Bond et al., 2004; Saikawa et al., 2009). Polycyclic Aromatic Hydrocarbons (PAHs) and their oxidative derivatives (Nitrated PAHs and Oxygenated PAHs) are one class of species with high toxic potency (Zhang et al., 2009; Jia et al., 2011; Wang et al., 2011a). PAHs released in the atmosphere come from both natural and anthropogenic sources; anthropogenic emissions include incomplete combustion of fossil fuels, agricultural burning, industrial and agricultural activities and are considered predominant (Ravindra et al., 2008; Zhang et al., 2009; Poulain et al., 2011; Kim et al, 2013; Abbas et al., 2018); natural contributions such as volcanic eruptions and forest fires are reported to be a less significant contributor to total emissions (Xu et al., 2006; Abbas et al, 2018).

Vapour phase PAHs can undergo gas phase reactions with oxidants in the atmosphere (including hydroxyl, ozone and nitrate radicals) leading to the generation of a range of nitrated-PAHs and oxygenated-PAHs (Atkinson et al., 1990; Atkinson and Arey., 1994; Sasaki, 1997). Atmospheric reaction with chlorine atoms in the presence of oxygen has also been suggested as a new formation pathway of OPAHs (Riva et al., 2015). OPAHs and NPAHs are often more toxic than the parent PAHs, showing a direct-acting mutagenicity on human cells (Durant et al., 1996; Hannigan et al., 1998; Purohit and Basu, 2000; Wang et al., 2011a; Benbrahim et al., 2012). Beside their formation in the gas phase, OPAHs and NPAHs can also be produced by heterogeneous reactions (Ringuet et al., 2012a, Jariyasopit et al., 2014; Zimmermann et al., 2013; Wenyuan et al., 2014; Keyte et al., 2013). Many of these derivatives can also be linked to primary emissions from motor vehicles and combustion processes (Rogge et al., 1993, Albinet et al., 2007a; Jakober et al., 2007; Shen et al., 2012; Nalin et al., 2016).

Many studies in different countries have focused on studying toxic organic pollutants in $PM_{2.5}$ because they fall within the respirable size range for humans (Sharma et al., 2007; Ringuet et al., 2012b, Farren et al., 2015). In the last decade, a major focus has been given to Chinese cities such as Shanghai, Beijing, Guangzhou, Tianjin, and Shenzhen because of their population growth and geographic peripheral expansion in manufacturing capacity and energy industries which are located throughout each of the city's manufacturing zones.
This has made China the world leader in energy consumption, but also the world's highest emitter of $PM_{2.5}$ and PAHs (Lin et al., 2018; Zhang et al., 2009; Xu et al., 2006). The majority of previous studies have reported PAH concentrations in 24 h averaged samples during short-term and long-term measurements campaigns (Tomaz et al., 2016; Alves et al., 2017; Niu et al., 2017; Benjamin et al., 2014; Wang et al., 2011a). However, a long averaging period creates some limitations such as sampling artefacts, notably where changing atmospheric photolysis conditions (air humidity, temperature, wind direction, ozone or other oxidant concentrations) may have a significant influence on PAHs concentrations and oxidation rates (Albinet et al., 2007b; Albinet et al., 2009, Goriaux et al., 2006, Tsapakis and Stephanou., 2003; Tsapakis and Stephanou., 2007, Ringuet et al., 2012b). More intensive and higher frequency measurements in field campaigns have been suggested as a means to improve the positive matrix factorization model performance (Tian et al., 2017, Srivastava et al., 2018). A few studies have used twice daily (12 h) sampling (Albinet et al., 2008; Zhang et al., 2018; Farren et al., 2015; Ringuet et al., 2012b), obtaining limited information on variability in concentrations during the daytime and night-time (Tsapakis and Stephanou., 2007). Shorter time periods for sampling (3 h and 4 h) are still very limited (Reisen and Arey., 2004; Srivastava et al., 2018). Considering the above, this paper determines the

76 temporal diurnal and nocturnal variation of the $PM_{2.5}$-bound concentrations of PAHs, OPAHs and NPAHs from

77 the air of Beijing in China, it shows the role of photochemistry in the formation of OPAHs and NPAHs and

78 associate the fate and evolution of PAHs, OPAHs and NPAHs with the gas phase concentrations of other

79 pollutants (O_3, CO, NO, NO_2, SO_2, HONO), the cancer risk associated with inhalation of $PM_{2.5}$ was calculated.

80 This paper explores the feasibility of higher frequency sampling in Beijing, to support the identification of

81 emissions sources from diagnostic ratios and correlations with atmospheric gas pollutants. These measurements

82 also raise the potential importance of the chemical relationship between NPAHs and HONO which may impact

83 the HONO budget in the atmosphere and, if included, improve related models. This study comes after three

84 years of declaring the anti-pollution action plan and strategy taken by the municipal government of Beijing and

85 published in September 2013 (Ministry of Ecology and Environment The People's Republic of China, Beijing

86 toughens pollution rules for cleaner air, 2013), trying to increase the number of days with good air quality index

87 by prohibiting coal combustion, promoting clean energy vehicles and public transport and helping industrial

88 transformation and upgrading to new technologies.

89

2 Experimental Steps

2.1 Sampling site and method

92 The sampling setup shown in Fig. S1 was located at the Institute of Atmospheric Physics, Chinese Academy of

93 Sciences in Beijing (39°58'28" N, 116°22'15" E) as part of the Air Pollution and Human Health (APHH)

94 research programme. $PM_{2.5}$ filter samples were collected on the roof of a 2-storey building about 8m above

95 ground level using a High-Volume Air Sampler (Ecotech HiVol 3000, Victoria, Australia) operating at 1.33 m^3

96 min^{-1}. Daytime particles were collected every three-hours during high PM concentration levels, nine-hours at

97 low PM levels and over 15 h at night-time during 18 continuous days (22 November 2016 to 9 December 2016).

98 Fifty-seven samples in total were collected. The daytime sampling started at 8:30 in the morning and the filter

99 was changed every 3 h. During low particulate loading conditions, the daytime sampling started at 8:30 in the

100 morning for a sampling duration of 9 h. Night-time sampling began at ~17:30 and ended at 08:30 the following

101 day. Prior to sampling, the quartz filters (20.3 × 25.4 cm) (supplied by Whatman (Maidstone, U.K.)) were baked

102 at 550 °C for 5 h in order to eliminate any organic matter. After sampling, filters were wrapped in aluminium

103 foil, sealed in polyethylene bags and stored at -20 °C until extraction and analysis.

104

2.2 Extraction method and clean up

106 All collected samples were extracted using an Accelerated Solvent Extractor automated system (Dionex, ASE

107 350). Prior to extraction, $1/16^{th}$ (surface area equivalent to 25.7 cm^2) of each filter was cut using a hole puncher

108 (Ø=27 mm) and for each batch of 6 samples, one sample was spiked with a mixture of two deuterated-PAHs

109 (Phenanthrene-D10; Pyrene-D10), two deuterated-OPAHs (9-Fluorenone-D8; 9,10-Anthraquinone-D8), and two

110 deuterated-NPAHs (1-Nitronaphthalene-D7; 3-Nitrofluoranthene-D9), as surrogate standards for PAHs, OPAHs

111 and NPAHs, respectively, with concentration on filters corresponding to 400 ng (40 µl, 10 ng $µl^{-1}$ in

3

112 Acetonitrile). All punched samples were cut to small pieces and packed into 5 mL stainless steel extraction cells.

113 Extractions were carried out in acetonitrile as follows: Oven at 120°C, pressure at 1500 psi, rinse volume 60%

114 and 60 s purge time for three consecutive 5 min cycles. Extracts (V=20ml) were evaporated to approximately 6

115 mL under a gentle stream of nitrogen before the clean-up step. All samples and blanks were purified on a SPE

116 silica normal phase cartridge (1g/6ml; Sigma Aldrich) to reduce the impacts of interfering compounds in the

117 matrix and to help maintain a clean GC injection inlet liner. After the clean-up step, the solution of each sample

118 was evaporated to 1 mL under a gentle stream of nitrogen at room temperature (20°C) and transferred to 1.5 mL

119 autosampler amber vial. Each concentrated sample was stored at 4°C until analysis. The average recovery

120 efficiencies calculated from surrogate standards ranged from 85% to 96% (Phenanthrene-d10: 95 ± 9 %; Pyrene-

121 d10: 101 ± 7 %; 9-Fluorenone-d8: 98 ± 13 %; 9,10-Anthraquinone-d8: 102 ± 11 %; 1-Nitronaphthalene-d7: 93

122 ± 8 %; 3-Nitrofluoranthene-d9: 101 ± 11 %) and the target compounds concentrations were calculated

123 incorporating measured recovery efficiencies.

124 **2.3 Chemical standards**

125 The chemical compounds that have attracted the most attention in previous studies are the 16 priority PAHs and

126 their derivatives, defined by the United States Environment Protection Agency (EPA). The choice of the organic

127 compounds investigated in this study is based on those associated with the particle phase and commercially

128 available standards. All compounds are listed in Table 1 and were purchased from Sigma Aldrich, Alfa Aesar

129 and Santa Cruz Biotechnology in the UK and had a minimum purity of 98%. In parallel to individual standards,

130 a mixed solution of the 16 EPA PAHs (CRM47940, Supelco, Sigma Aldrich) of 10 µg ml^{-1} in acetonitrile was

131 also used. Standard solutions for calibrations were prepared in acetonitrile (HPLC grade, 99.9% purity, Sigma

132 Aldrich). Deuterated compounds were supplied by C/D/N isotopes and distributed by QMX Laboratories Ltd

133 (Essex, UK).

134 **2.4 GC/MS Analysis**

135 Target compounds were quantified using a GC - accurate mass Quadrupole Time-of-Flight GC/MS system (GC

136 Agilent 7890B coupled to an Agilent 7200 Q-TOF-MS). Parent PAHs were separated in a 35 min analysis time

137 using a capillary HP-5MS Ultra Inert GC column (Agilent; 5%-Phenyl substituted methylpolysiloxane; length:

138 30 m, diameter: 0.25 mm, film thickness: 0.25 µm). Inlet injections of 1 µL were performed in pulsed splitless

139 mode at 320 °C using an automated liquid injection with the GERSTEL MultiPurpose Sampler (MPS). Helium

140 was used as a carrier gas at 1.4 mL min^{-1}. The GC oven temperature was programmed to 65 °C for 4 min as a

141 starting point and then increased to 185 °C at a heating rate of 40 °C min^{-1} and held for 0.5 min, followed by a

142 heating rate of 10 °C min^{-1} to 240 °C and then ramped at 5 °C min^{-1} until 320 °C and held isothermally for

143 further 6 min to ensure all analytes eluted from the column. The MS was operated in Electron Ionisation (EI)

144 mode at 70 eV with an emission current of 35 µA. Calibration solutions were injected 3 times in the same

145 sequence for samples and covered the range from 1pg µL^{-1} to 1000 pg µL^{-1}.

146 The method development for OPAHs and NPAHs was based on previous studies (Albinet et al., 2006; Albinet

147 et al., 2014; Bezabeh et al., 2003; Kawanaka et al., 2007) using Negative Chemical Ionisation (NCI) performed

148 at 155 eV and 48 µA, with methane (CH$_4$, research grade 5.5, Air Liquide) as reagent gas. Target compounds

149 were eluted using the RXi-5ms (Restek GC column) with similar phase and characteristics to HP-5ms. Analysis

150 was performed in 29.2 min and the GC settings were as follows: 1 µL of each sample was injected in pulsed

151 splitless mode at 310 °C, Helium flow was set to 1.2 mL min^{-1}, the initial oven temperature of 70 °C was held

152 for 4 min, followed by a heating rate of 60 °C min^{-1} until 190 °C and then raised to 270 °C at rate of 25 °C min^{-1}

153 and ended with 5 °C min^{-1} until 320 °C, held for 10 min. A 10-point calibration curve within the range 0.5 pg

154 µL^{-1} to 1000 pg µL^{-1}, was obtained with the correlation coefficients from the linear regression from 0.980 to

155 0.999.

156

157 **2.5 Data analysis and error evaluation**

158 Data acquisition were recorded and processed using the Agilent Qualitative and Quantitative analysis software.

159 Target compounds were isolated using Extracted-Ion Chromatograms (EIC) and identified by the combination

160 of retention time and mass spectral match against the calibration standards measured simultaneously within the

161 samples. The limit of detection (LOD) was defined as the valid lowest measurable peak response to peak noise

162 near the elution time of the target peak (S/N = 3) in a mix of standards solutions. As the chemical noise

163 increases during the analysis of real samples the Limit of Quantification (LOQ) was defined S/N=10. These

164 recommendations are in accordance with previous analytical studies (Nyiri et al., 2016; Ramírez et al., 2015).

165 LOD values were evaluated from standards solutions and ranged between 1 pg and 20 pg for PAHs, 0.01 pg and

166 0.2 pg (except 1-naphthaldehyde 0.5 pg) for OPAHs and 0.02 pg to 0.25 pg for NPAHs.

167 To determine any sources of contamination during sample preparation and the analytical procedure, the solvent

168 (acetonitrile) and field blanks (n=2) were analysed following the same procedure as for the samples (Extraction,

169 SPE, Evaporation). Most target compounds were found to be below LOD (S/N=3) or orders of magnitude (up to

170 10^3 - 10^4) lower than was found in the samples. A small number of compounds found in field blanks (1,8-

171 Naphthalic anhydride, Benzo[a]fluorenone, 1-Nitronaphthalene, 9-Nitroanthracene) have a higher contribution

172 (4-30 %) to very few filters (2 to 5 samples) collected over a 3 h time period, if this was co-incident with low

173 particulate loading conditions. The contribution to each compound from field blanks has been corrected in the

174 final data.

175 We evaluated the precision of the method by calculating the relative standard deviations (%RSD) from replicate

176 analysis as shown in Table 1. For PAHs, the precision of sample replicates (n=10) during inter-day and intra-

177 day varied from 1.8% to 8.9% (mean 5.2%) and 1.2% to 8.7% (mean 3.4%), respectively. The %RSD average

178 for deuterium labelled compounds was about 3.6%. For OPAHs and NPAHs, two different concentrations of

179 standards were analysed (50 pg; n=6 and 400 pg; n=6); inter-day precision of 10 OPAHs gives an average

180 %RSD of 6.8% (range: 5.4 - 8.9%) and intra-day precision of 5.6% (3.2 - 7.8%). Similar to OPAHs,

181 repeatability and reproducibility between days for NPAHs varied from 3.9% to 8.4% (mean 5.5%) and 3.2% to

182 9.7% (mean 5.2%), respectively. Hence, the estimated random error quantified by the standard deviation of the

183 measurements did not exceed 7% on average. The systematic error may be due to the influence of the sample

184 matrix during the analysis sequence on the quantification step and the calibration offset. It was estimated to be a

185 maximum 10% from the measured recovery of the deuterium species (Garrido-Frenich et al., 2006). Therefore,

186 the overall estimated error, combining the precision and the systematic effects, is less than 20%.

187 Another source of error can be attributed to sampling artefacts and this has been discussed in previous studies
188 (Schauer, C. et al., 2003, Goriaux, M. et al., 2006, Tsapakis and Stephanou, 2003). The absence of an ozone
189 denuder to trap the gas phase oxidants may lead to an underestimation of the true values of PAHs due to
190 chemical decomposition. Therefore, data from long sampling times and under high ozone ambient
191 concentrations may be biased by sampling artefacts by more than 100 % (Schauer et al., 2003, Goriaux et al.,
192 2006). However, at low ozone levels, negative artefacts were considered not significant (Tsapakis and
193 Stephanou 2003), whilst, at medium ozone levels (30-50 ppb) PAHs values were underestimated by 30 %
194 (Schauer et al., 2003). In addition, heterogeneous reactions during particle sampling may occur only on the
195 monolayer surface coverage with limited diffusion of oxidants to the bulk particles (Keyte et al., 2013 and
196 references therein). Previous studies reported that the formation of NPAHs during high-volume sampling is not
197 significant and calculated to be < 3 % (Arey et al., 1988) and < 0.1 % (Dimashki et al., 2000).

198 Considering the role of ozone (always below 30 ppb in this study, with a mean value: 10.4 ± 8.8 ppb), in
199 addition to sampling time and temperature, the estimation of the negative sampling artefacts on our data range
200 between 10 and 20 %, with the highest error estimation attributable to longest sampling time (15h).

201 **3 Results and discussion**

202 **3.1 Temporal variations of PAHs, OPAHs and NPAHs in $PM_{2.5}$**

203 The volume of literature on $PM_{2.5}$ has rapidly increased over the last two decades and various disciplines have
204 contributed to improve understanding about source emissions, chemical composition, and impact on people's
205 behaviour and health. In China, the official air quality guidelines for $PM_{2.5}$ expressed as annual mean and 24 h
206 average are 35 µg m^{-3} and 75 µg m^{-3}, respectively (WHO 2016; Ministry of Ecology and Environment The
207 People's Republic of China, 2012). During the sampling period of this study (Nov - Dec 2016), $PM_{2.5}$ was
208 measured every hour and ranged from 3.8 to 438 µg m^{-3}, with an average concentration of 103 µg m^{-3}. The
209 average 24 h $PM_{2.5}$ concentration was 108 ± 82 µg m^{-3} (range: 10 - 283 µg m^{-3}), exceeding the 24 h limit value
210 on 10 of the 18 sampling days. Concurrent $PM_{2.5}$ concentrations were averaged to the filter sampling times (3 h,
211 9 h, 15 h) and are shown in Fig.6 and Fig. S3. The daily (24 h) concentration of Benzo[a]pyrene ranged from
212 4.46 to 29.8 ng m^{-3} (average 15 ± 8.9 ng m^{-3}), exceeding the 24 h average limit value of 2.5 ng m^{-3} for China
213 (Ministry of Ecology and Environment The People's Republic of China, 2012) on all of the 18 days of sampling
214 period.

215 Fig. 1 shows the measured concentrations of PAHs in the 3 h daytime samples ranging from 18 to 297 ng m^{-3}
216 (average 87.3 ± 58 ng m^{-3}) and from 23 to 165 ng m^{-3} (average 107 ± 51 ng m^{-3}) in the 15 h night-time samples.
217 The 24 h total concentrations (combined results from daytime and night-time samples) of the 16 PAHs varied
218 between 37 and 180 ng m^{-3} (average 97 ± 43 ng m^{-3}). PAHs derivatives showed the following trends: total
219 OPAHs concentrations varied from 3.3 to 55 ng.m^{-3} (average: 26 ± 16 ng m^{-3}) in daytime and from 8.9 to 95 ng
220 m^{-3} (average: 41.6 ± 26 ng m^{-3}) at night-time; OPAHs were approximately 25 and 14 times higher than average
221 NPAHs in the daytime (average: 1.03 ± 0.74 ng m^{-3}, range: 0.13-2.3) and night-time (average: 3.06 ± 1.8 ng m^{-3},
222 range: 0.57-6.43), respectively.

PHE (See Table 1 for abbreviations), FLT, PYR, BaA, CHR, BbF and BaP were the largest contributors to the total PAH concentration. 9-FLON, 9,10-ANQ and 1,8-NANY were the three major O-PAHs species. The most abundant NPAHs were 3-NDBF, 9-NANT and 3-NFLT. The temporal profile and contributions of each compound to the total concentration are shown in Fig. 2 and detailed in Table 2. The highest concentrations recorded in this study were in the day of 29 Nov 2016; concentrations of all target compounds in the particulate phase are displayed in Fig. S2. Some nitro-compounds (5-NAC, 1-NPYR, 6-NCHR, 6-NBaP) were below LOQ in a few samples while one oxy-compound (1,8-Naphthalic anhydride) was outside the dynamic range and limit of linearity of the calibration curve for samples with high mass loading (Table 2). Similar dominant compounds were found in different urban cities (Xi'an, Jinan, Beijing) of China (Bandowe et al. 2014, Zhang et al. 2018, Wang et al., 2011c). The average 24 h total PAH concentrations (97 ng m^{-3}) in this study was higher than the average value reported for Guangzhou city in the south of China (average 45.5 ng m^{-3}, from Liu et al., 2015), however, it was lower than average values reported for Xi'an city in winter (range 14-701 ng m^{-3}; average 206 ng m^{-3} from Wang et al., 2006) and in the suburb of Beijing in winter (average 277 ng m^{-3}, from Feng et al., 2005). Our average value (97 ng m^{-3}) was comparable to the reported values in a recent study (Feng et al., 2019) at the campus of Peking University health science centre, a short distance from our sampling site (~1 mile), where the authors reported a total PAHs average concentration in winter Beijing (2014 - 2015) of 88.6 ± 75 ng m^{-3}. The lower average concentration of total PAHs reported in this study and Feng et al., (2019) can potentially be attributed to the efforts from municipal government to improve air quality and control emissions by reducing combustion sources in the intervening years. The urban location in this study (Fig. S1) was surrounded by busy roads, residential buildings, an underground railway, restaurants and further afield thermal power stations. PAHs concentrations are anticipated to decline closer to the mountains in the North and West of Beijing due to air mass trajectory, aging and distance from emission sources. Results from this study can be considered representative (within the margin of error) of the urban area in Beijing including districts such as Chaoyang, Haidian, Fengtai, Xicheng, Dongcheng, Shijingshan covering an approximate population of 12 million. Future studies in less populated districts and different areas of the metropolitan of Beijing would be helpful for comparison of population exposures.

Concentrations of PAHs in PM$_{10}$ (range: 3.2 - 222.7 ng m^{-3}) in Beijing were found in previous studies to be lower than in PM$_{2.5}$ (Wang et al., 2011c). The concentration of PAHs in this study were much lower than reported in certain other megacities, for example, Delhi, India in winter season 2003 (range: 948-1345 ng m^{-3}; mean: 1157 ± 113 ng m^{-3} from Sharma et al., 2007) and Mexico City, Mexico in October 2002 (range: 60-910 ng m^{-3}; mean: 310 ng m^{-3} from Marr et al., 2004). Average concentrations for total PAH in the first 3 h filter of the day (8:30-11:30 am; Monday to Friday; mean: 112 ng m^{-3}) were 1.5 times higher than the rest of the day, and 1.6 times higher than the same first 3 h on a Sunday. A potential reason of the elevated concentrations in the morning hours is due to the rush hour traffic during working days, coupled to a period of shallow boundary layer.

The mean total concentrations in Table 2 for the 3 h integration samples of OPAHs and NPAHs were 28.7 ± 21 ng m^{-3} (range: 1.8 - 87.9 ng m^{-3}) and 1.17 ± 1 ng m^{-3} (range: 0.15 - 3.92 ng m^{-3}). Average night-time was 41.6 ng m^{-3} (OPAHs) and 3.06 ng m^{-3} (NPAHs), concentrations which were 2.6 and 35 times lower than the average total PAH in the night samples. The ratios of mean concentrations of PAH divided by concentration of OPAH

263 and NPAH for the 3 h samples were 3 and 74. Ratios of combined daytime and night-time samples (24 h) were

264 on average 2.9 (range 1.9 - 4.6) for ∑PAHs/∑OPAHs and 47.4 (range 25 - 79) for ∑PAHs/∑NPAHs. Lower

265 ratios were reported from a winter study in Xi'an – China, where ∑PAHs/∑OPAHs ranged from 1.75 to 1.86

266 and ∑PAHs/∑NPAHs ranged from 34 to 55.2. On the other hand, similar trends to our study were recorded for

267 ∑PAHs/∑OPAHs in Europe such as Athens in Greece in winter (ratio 28.9/6.9 = 4.2) (Andreou and

268 Rapsomanikis., 2009) and Augsburg in Germany in winter (ratio 11/3.2 = 3.4) (Pietrogrande et al., 2011).

269 Further monitoring studies are needed to confirm trends of NPAHs in China.

270

271 **3.2 Diagnostic ratios to identify emission sources**

272 The concentration ratios between different PAHs are widely used to assess and identify pollution emission

273 sources (Tobiszewski and Namieśnik., 2012 and references therein). The ratios of FLT/(FLT + PYR) and

274 IcdP/(IcdP + BghiP) isomer pairs are commonly used to distinguish between emission sources such as

275 coal/biomass burning or the incomplete combustion of petroleum. Values of FLT/(FLT + PYR) and IcdP/(IcdP

276 + BghiP) higher than 0.5 indicate dominance of a coal/biomass burning source. Values of FLT/(FLT + PYR)

277 between 0.4 and 0.5 and IcdP/(IcdP + BghiP) between 0.2 and 0.5 suggest a higher influence from fossil fuel

278 combustion. Values of FLT/(FLT + PYR) less than 0.4 and IcdP/(IcdP + BghiP) less than 0.2, are mostly related

279 to incomplete combustion (petrogenic origin) (Yunker et al., 2002; Pio et al., 2001). The measured ratios in this

280 study are shown in Fig. 3 and ranged from 0.53 to 0.67 (mean 0.56) during the day (3 h and 9 h samples), while

281 at night (15 h samples) varied between 0.51 and 0.54 (mean 0.52) indicating primary emissions from coal and

282 biomass burning. Lower values were observed for IcdP/(IcdP + BghiP); daytime ratios were between 0.39 and

283 0.5 (3 h and 9 h samples) indicated the dominance of petroleum combustion. At night, the ratio in most samples

284 was slightly higher than 0.5, with some values below, suggesting mixed sources with likely higher contributions

285 coming from residential heating using coal and wood at night.

286 As shown in Fig. 4, other ratios can be useful to confirm the contribution from local traffic and to discriminate

287 vehicle emissions such as BaP/BghiP, FLU/FLU+PYR and BaP/BaP+CHR (Tobiszewski and Namieśnik., 2012

288 and references therein). The BaP/BghiP ratios were significantly higher than 0.6 indicating a major influence

289 from road traffic, while FLU/FLU+PYR ratios suggested a predominant petrol contribution (ratio < 0.5) instead

290 of diesel engines (ratio > 0.5). Results shown in Fig. 4 identify traffic emissions and in particular petrol engines

291 as the major emitter of PAHs. In PM$_{2.5}$, the 5- and 6-rings PAHs species (BaP, IcdP, BghiP) were previously

292 attributed to petrol engines, while lower molecular weight with 3-rings (ACY, AC, FLU, PHE, ANT) and 4-

293 rings (FLT, PYR, BaA, CHR) were closely related to diesel vehicle emissions (Chiang et al., 2012; Wu et al.,

294 2014 and references therein). Previous studies in Beijing and Guangzhou in China suggested similar

295 contributions from coal and petroleum combustion, focusing on vehicular traffic (petrol and diesel) as potential

296 sources for PAHs (Gao and Ji., 2018; Liu et al., 2015; Wu et al., 2014, Niu et al., 2017).

297 NPAHs can be used to track the photochemistry of PAHs with OH and NO$_3$ radicals, both of which can generate

298 secondary photochemical products of NPAHs and OPAHs from primary PAH emissions (Zhang et al., 2018;

299 Ringuet et al., 2012b; Wang et al., 2011a). 1-NPYR originates mainly from primary emissions and in particular

300 from diesel vehicles (Keyte et al., 2016, Schulte et al., 2015), whilst 2-NFLT has been reported to be absent in

direct combustion emissions, instead produced from the gas-phase reactions of FLT with OH radicals in presence of NOx during the day or NO$_3$ radicals at night. 2-NPYR comes solely from the reaction of PYR with OH radicals (Ramdahl et al., 1986; Arey et al., 1986; Atkinson et al., 1987; Ciccioli et al., 1996). Accordingly, the ratio 2-NFLT/1-NPYR has been widely used as diagnostic, with a value greater than 5 indicating a major contribution from photochemical processes, whilst a ratio value less than 5 means an important contribution from direct emissions (Albinet et al., 2008; Wang et al., 2011a; Ringuet et al., 2012b; Bandowe et al., 2014; Tomaz et al., 2017; Zhang et al., 2018).

In this study, the 2-NFLT was not quantified because the standard compound was not commercially available, subsequently, we have used 3-NFLT isomer as a substitution of 2-NFLT. PAH isomer pairs (Table 1) in standard mixtures showed similar sensitivities for each concentration used, therefore, we assume an equal sensitivity for 2-NFLT and 3-NFLT during analysis. A previous study reported that the concentration of 3-NFLT compared to 2-NFLT is relatively very low in ambient air (Bamford et al., 2003); in addition, the separation of both isomers (2- and 3-NFLT) using the most common GC-MS column for PAHs separation, HP-5ms and DB-5ms, was not possible (Zhang et al., 2018; Bandowe et al., 2014; Ringuet et al., 2012b; Albinet et al., 2008). Hence, we assume that the sum of 2- and 3-NFLT is closely representative of the original ratio 2-NFLT/1-NPYR. Therefore, we adopted the ratio 2+3NFLT/1-NPYR, which varied between 4 and 19 during the daytime (mean: 12) and from 3.6 to 30.4 in the night-time (mean: 8.8) (Fig. S3). Most daytime values exceeded significantly the benchmark ratio of 5, while at night-time the average value was lower. These results indicate the predominance of OH-radicals-initiated reactions controlling the formation of 2-NFLT in presence of NO$_2$ and sunlight.

3.3 Correlation with gaseous pollutants

O$_3$, CO, NO, NO$_2$, SO$_2$ and HONO were also measured at the same site location as the PM$_{2.5}$ sampling. Inlets were installed outside lab containers at approximately 3-4 m above ground (Fig. S1). Online measurements of the gas phase species have been time-averaged to the filter sampling times. No correlations of significance were seen between PAHs and meteorological parameters (Relative Humidity and Temperature) as shown in Table S1.

∑PAHs and ∑OPAHs had a similar strong positive correlation (R= 0.82 to 0.98) in the 9 h and 15 h samples with CO, NO, NO$_2$, SO$_2$ and HONO (Table S1). NO is known as an effective tracer for local traffic emissions, it and behaves as a short-lived intermediate (Bange 2008, Janhäll et al., 2004). CO is mainly produced from incomplete combustion and has a relatively long atmospheric lifetime (3 months on average) and undergoes long-range transport (Peng et al., 2007 and references therein). The high correlations with primary pollutants such as NO and CO during the daytime and night-time indicate that PAHs and OPAHs are primarily emitted from local sources may also be associated with regional scale emissions. Significant correlations were observed with SO$_2$, a pollutant mostly emitted from power plants outside the city (Lee et al., 2011). This strong relationship with SO$_2$ could be explained by the contribution of anthropogenic sources such as the Beijing Taiyanggong thermal power station (39°58′42″N 116°26′19″E), and is consistent with the domain air masses arriving at the sites from the North East for much of the time (Fig. S4).

In contrast, most of the 3 h day samples showed only moderate correlations (R=0.38 to 0.74) except for HONO where significant correlations (R=0.87 to 0.94) were observed with ∑PAHs, ∑OPAHs and ∑NPAHs (Fig. 5;

Table S1). Furthermore, HONO was significantly correlated with $PM_{2.5}$ during the daytime (Fig. 5) and some significant chemical link between HONO emissions and ambient particles ($PM_{2.5}$) is implied. A similar conclusion was drawn from recent study in Beijing (Zhang et al., 2019) which suggested a potential chemical relationship between HONO and haze particles ($PM_{2.5}$) and proposed a high contribution from vehicle emissions to the night-time HONO.

For NPAHs, as shown in Table S1, no significant correlation was found in 3 h and 15 h time sampling resolution, except with HONO, where a significant difference between day and night were observed. Surprisingly, the 9 h time resolution showed a strong correlation with CO, NO, NO_2 and SO_2, potentially suggesting a direct emission of NPAHs. More likely these correlations arise because of a formation delay of NPAHs that is smoothed out by the longer daytime sampling period. In a previous study, Zimmermann et al., (2013) reported the formation of NPAHs from the heterogeneous interaction of ambient particle bound-PAHs with atmospheric oxidant. In line with the observed high values for the ratio 2+3NFLT/1-NPYR (section 3.2) and the trace levels of NPAHs concentrations in the atmosphere; the secondary formation of NPAHs by gas phase reactions followed by adsorption on particles and in parallel the heterogeneous formation on the surface of particles is supported rather than primary emissions.

HONO plays a key role in tropospheric photochemistry, however its sources and their relative contributions to ambient HONO are still unclear, especially in the daytime. To help understand the mechanism of HONO formation in the atmosphere, each NPAHs compound has been correlated with HONO concentrations. The available data in Table S2 shows diurnal and nocturnal differences for individual correlation of NPAHs with HONO with the exception for 1-NPYR, which originates mainly from primary emissions and shows a strong correlation during the day and night. 9-Nitroanthracene had distinctive behaviour, accumulating during the night and appearing to undergo a photo-degradation during the daytime (Fig. 6). As shown in Table S2, 9-Nitroanthracene showed a strong positive correlation with HONO (R=0.90, P<0.001) in the daytime while no significant relationship was found at night-time (R=0.15, P>0.05). This suggests 9-nitroanthracene as a possible source of HONO during the daytime via the OH radical-initiated reaction leading to OH (ortho) addition and followed by intramolecular hydrogen transfer from the phenolic hydroxyl group to the nitro group.

There was a significant positive correlation between ANT and 9-NANT (R= 0.90, 3 h; R=0.94, 9 h; R=0.90, 15 h; P≤0.001), which may be an indication that 9-NANT is closely related to ANT. In this respect, additional simulation chamber measurements of the gas phase reaction of ANT with NO_3 radicals and for 9-Nitroanthracene with OH radicals in presence of light and under different atmospheric parameters are required for more precise assessment.

3.4 Exposure assessment

The toxicity equivalency factor (TEF) represents an estimate of the relative toxicity of a chemical compared to a reference chemical. For PAHs, Benzo[a]pyrene was chosen as the reference chemical because it is known as the most carcinogenic PAH (OEHHA., 1994, 2002) and is commonly used (Albinet et al., 2008; Tomaz et al., 2016; Alves et al., 2017; Bandowe et al., 2014; Ramírez et al., 2011) as an indicator of carcinogenicity of total PAHs.

376 The toxicity of the total PAHs expressed as BaP equivalents (BaP_{eq}) is calculated from the TEFs of each target

377 compound (Table S3) multiplied by its corresponding concentration Eq. (1):

$$\sum [BaP]_{eq} = \sum_{i}^{n=1} (C_i \; x \; TEF_i) \qquad (1)$$

379 where C_i correspond to the concentration of individual target compound (PAHs, OPAHs and NPAHs) in ng m^{-3}.

380

381 A widely applied procedure from the Office of Environmental Health Hazards Assessment (OEHHA) of the

382 California Environmental Protection Agency (CalEPA) and also the World Health Organisation (WHO) was

383 used here to evaluate and calculate the potential of contracting cancer from inhalation and exposure to PM$_{2.5}$-

384 bound PAHs; commonly known as the lifetime excess cancer risk (ECR) Eq. (2).

$$ECR = \sum [BaP]_{eq} \times UR_{BaP} \qquad (2)$$

386

387 where two values are mostly used for UR$_{[BaP]}$ (1.1×10^{-6} (ng m^{-3})$^{-1}$ (OEHHA., 2002, 2005) and 8.7×10^{-5} (ng m^{-3})$^{-1}$

388 (WHO., 2000)); Eq. (2) describes the inhalation unit risk associated with high probability of contracting cancer

389 when exposed continuously to 1 ng m^{-3} of BaP_{eq} concentration over a lifetime of 70 years.

390 As shown in Table 3, the BaP_{eq} concentration includes the sum of 16 PAHs, 1 OPAH and 6 NPAHs, with the

391 cancer risk evaluated using different sampling times according to CalEPA and WHO guidelines. The risk values

392 may be underestimated due to lack of toxicity data for OPAHs and because our assessment excludes the gas

393 phase contributions i.e. are only based on the health risk evaluation of the particulate phase. The average 24 h

394 BaP_{eq} for the whole sampling period was 23.6 ± 12.4 ng m^{-3} (Table 3). As shown in Table 2, 6-NCHR has not

395 been quantified in all samples, its contribution to the total BaP_{eq} is relatively high (mean: 8%, range: 1 - 24%) in

396 comparison with the three major contributor from the PAH group: BaP (mean: 47.5%, range: 24 - 64%), DahA

397 (mean: 17.8%, range: 10 - 32%) and BbF (mean: 10.1%, range: 7 - 21%). In this study, the ECR attributable to

398 all polycyclic aromatic compounds (PACs) in urban air of Beijing ranged from 10^{-5} to $10^{-3} > 10^{-6}$ (Table 3)

399 suggesting an elevated potential cancer risk for adults (Chen and Liao., 2006; Bai et al., 2009).

400 It is worth noting that inhalation exposure is not the only risk related to PAHs and cancer in humans. Other

401 sources of exposure include dermal contact and ingestion of the re-suspended dusts in matrices such as road

402 dusts and soils all of which increase the risk value for urban residents (Wang, et al., 2011b; Wei et al., 2015). In

403 this study, the 24 h average estimated cancer risk (Table 3) from inhalation exposure to ambient PM$_{2.5}$ based on

404 CalEPA and WHO guidelines were 2.6×10^{-5} and 2.05×10^{-3}, respectively. Using the highest calculated ECR

405 (2.05×10^{-3}) gives an estimate of 2027 additional cancer cases per million people exposed (29 cases/year) in

406 comparison to the estimate based on CalEPA of 26 persons (0.37 cases/year).

407 ECR trends were reported in previous studies from Beijing and other populated area (Bandowe et al., 2014;

408 Alves et al., 2017; Ramírez et al., 2011; Jia et al., 2011, Liu et al., 2015, Song et al., 2018, Feng et al., 2019). In

409 this study we considered the combination of all samples (n=54) to estimate the average 24 h cancer risk

($\sum[BaP]_{eq}$=23.6 ± 12 ng m^{-3}; range 8 – 44 ng m^{-3}) and compare it with previous studies. An average value of 17 ng m^{-3} (range 2-64 ng m^{-3}) was reported for Xi'an for the whole year between July 2008 and August 2009 (Bandowe et al., 2014). After considering the same winter period (November and December) as in our study, the average values reported for Xi'an city (31-33 ng m^{-3}) were higher than our results. In contrast, our average value was comparable to those reported in a recent study in Beijing, ranging from 21 to 38 ng m^{-3} in cold months (Feng et al., 2019), whilst in the previous study of Chen et al. 2017, they reported an average of 31.4 ng m^{-3} for outdoor air in Beijing in winter. Lower and more varied values have been also reported in Beijing in winter. Liu et al. (2007) reported an average BaP_{eq} concentration of 13.0 ng m^{-3} and 27.3 ng m^{-3} at two sampling sites on Peking University campus and 82.1 ng m^{-3} for samples collected from busy road street. It is clear that direct comparison with Beijing air from other studies is limited due to the variable number of compounds considered in each study and the differences in sampling sites and sampling periods. Other areas of uncertainty include TEF reference values and the range of BaP UR which were extrapolated from animal bioassays with limited evidence regarding the carcinogenicity to humans.

Seasonal variability is also crucial in estimating BaP_{eq} concentrations; it has been shown that BaP_{eq} values in cold months are always higher than warm months due to the increase in coal combustion, central and residential heating, lower photochemical transformation and lower volatilisation of gases favouring particle formation in winter. Previous observations in Beijing recorded $\sum[BaP_{eq}]$ of 11.1 ng m^{-3} in autumn (Jia et al., 2011) and 11.0 ng m^{-3} in warm months (April to June) (Feng et al., 2019). In comparison with Guangzhou city (south of China), BaP_{eq} was 9.24 ng m^{-3} in winter and reported to be 1.6 and 6.2 times greater than autumn and summer, respectively (Liu et al., 2015). Our results were considerably higher than those estimated for western European cities during the winter, such as Grenoble: 1.4 ng m^{-3} (Tomaz et al., 2016), Oporto: 3.56 ng m^{-3}, Florence: 1.39 ng m^{-3} and Athens: 0.43 ng m^{-3} (Alves et al., 2017). ECR values estimated for each city were 31 (Grenoble), 6.6 (Oporto), 17 (Florence) and 54 (Athens) times lower than our ECR estimation. Lower ECR levels in western European cities were attributed to cleaner energy sources, less densely populated cities, waste exporting and recycling and more effective environmental regulations.

4 Conclusions

Temporal variations and chemical composition of PM$_{2.5}$ were measured in Beijing-China from 22 November 2016 to 9 December 2016, focusing in particular on the diurnal and nocturnal chemical formation of PAHs, OPAHs and NPAHs. The 24 h average concentration of PM$_{2.5}$ was 108 µg m^{-3} ranging from 10 to 283 µg m^{-3}, exceeding the 24 h limit value for China on 10 out of 18 sampling days. The 24 h concentrations of $\sum$PAH$_{16}$ varied between 37 and 180 ng m^{-3} (average 97 ± 43 ng m^{-3}), while $\sum$OPAH$_{10}$ ranged from 13 to 70 ng m^{-3} (average 35.6 ± 19 ng m^{-3}) and $\sum$NPAH$_9$ from 0.87 to 4.4 ng m^{-3} (average 2.29 ± 1.2 ng m^{-3}). Daytime concentrations during pollution episodes for PAHs, OPAHs and NPAHs were 224, 54, and 2.3 ng m^{-3}, respectively. The daily concentration of Benzo[a]pyrene exceeded the 24 h average limit value of 2.5 ng m^{-3} for China on all sampling days in this study, indicating elevated risk of disease among inhabitants.

Diagnostic ratios of different species were used to distinguish between possible emission sources of PAHs. Coal combustion and road traffic emissions (petrol engines) were found overall to be the two dominant sources. In addition, high ratios of 2+3Nitrofluoranthene/1-Nitropyrene indicated significant secondary formation of NPAHs, especially in daytime via the OH radical-initiated reaction pathway.

PAHs and OPAHs concentrations were correlated with CO, NO, NO_2, SO_2 and HONO, indicating that both are associated with local and regional primary emissions and in particular to traffic sources. Correlations seen previously between $PM_{2.5}$ and HONO suggested a possible links and a potential source of HONO that would affect the budget of HONO and OH radicals. The strong positive correlation between individual NPAHs and HONO during daytime was also suggestive of a potential link between these two classes of chemicals in air. One of the dominant NPAHs, the 9-Nitroanthracene had distinctive behaviour, accumulating at night and photodegrading in daytime.

The lifetime excess cancer risk attributable to the summation of polycyclic aromatic compounds measured here and associated with $PM_{2.5}$ inhalations in Beijing was in the range of 10^{-3} according to WHO guidelines, confirming that there is statistically elevated risk of contracting cancer from this class of pollutants in this location.

478 **References**

479 Arey, J., Zielinska, B., Atkinson, R., Winer, A. M., Ramdahl, T., Pitts Jr, J. N.: The formation of nitro-PAH
480 from the gas-phase reactions of fluoranthene and pyrene with the OH radical in the presence of NO$_x$,
481 Atmospheric. Environment., 20, 2339-2345, doi: 10.1016/0004-6981(86)90064-8, 1986.

482 Atkinson, R., Arey, J., Zielinska, B., Pitts Jr, J.N., Winer, A.M.: Evidence for the transformation of polycyclic
483 organic matter in the atmosphere, Atmospheric. Environment., 21, 2261–2262, doi:10.1016/0004-
484 6981(87)90357-X, 1987.

485 Arey, J., Zielinska, B., Atkinson, R., Winer. A.M.: Formation of nitroarenes during ambient high-volume
486 sampling, Env. Sci. Tech, 22, 457-462, doi:10.1021/es00169a015,1988.
487
488 Atkinson, R., Arey, J., Zielinska, B., Aschmann, S. M.: Kinetics and nitro-products of the gas-phase OH and
489 NO$_3$ radical-initiated reactions of naphthalene-d8, fluoranthene-d10, and pyrene, Int. J. Chem. Kinet., 22, 999–
490 1014, 1990.

491 Atkinson, R., and Arey, J.: Atmospheric chemistry of gas-phase polycyclic aromatic hydrocarbons: formation of
492 atmospheric mutagens, Environ. Health. Perspect., 102, 117–126, 1994.

493 Albinet, A.; Leoz-Garziandia, E.; Budzinski, H.; Villenave, E.: Simultaneous analysis of oxygenated and
494 nitrated polycyclic aromatic hydrocarbons on standard reference material 1649a (urban dust) and on natural
495 ambient air samples by gas chromatography-mass spectrometry with negative ion chemical ionisation, Journal.
496 of Chromatography. A., 1121, 106–113, doi:16/j.chroma.2006.04.043, 2006.
497
498 Albinet, A., Leoz-Garziandia, E., Budzinski, H., Villenave, E.: Polycyclic aromatic hydrocarbons (PAHs),
499 nitrated PAHs and oxygenated PAHs in ambient air of the Marseilles area (South of France): Concentrations
500 and sources, Science. of the Total. Environment., 384, 280–292, doi:10.1016/j.scitotenv.2007.04.028, 2007a.

501 Albinet, A., Leoz-Garziandia, E., Budzinski, H. and Villenave, E.: Sampling precautions for the measurement of
502 nitrated polycyclic aromatic hydrocarbons in ambient air, Atmospheric Environment, 41, 4988–4994,
503 doi:16/j.atmosenv.2007.01.061, 2007b.
504
505 Albinet, A., Leoz-Garziandia, E., Budzinski, H., Villenave, E., Jaffrezo, J. L.: Nitrated and oxygenated
506 derivatives of polycyclic aromatic hydrocarbons in the ambient air of two French alpine valleys Part 1:
507 Concentrations, sources and gas/particle partitioning, Atmospheric. Environment. 42, 43–54,
508 doi:10.1016/j.atmosenv.2007.10.009, 2008.

509 Albinet, A., Papaiconomou, N., Estager, J., Suptil, J. and Besombes, J.-L.: A new ozone denuder for aerosol
510 sampling based on an ionic liquid coating, Analytical and Bioanalytical Chemistry, 396, 857–864,
511 doi:10.1007/s00216-009-3243-5, 2009.
512
513 Andreou, G., Rapsomanikis. S.: Polycyclic aromatic hydrocarbons and their oxygenated derivatives in the urban
514 atmosphere of Athens, Journal. of Hazardous. Materials., 172, 363–373, doi:10.1016/j.jhazmat.2009.07.023,
515 2009.

Albinet, A.; Nalin, F.; Tomaz, S.; Beaumont, J.; Lestremau, F.: A simple QuEChERS-like extraction approach for molecular chemical characterization of organic aerosols: application to nitrated and oxygenated PAH derivatives (NPAH and OPAH) quantified by GC–NICIMS, Anal. Bioanal. Chem., 406, 3131–3148, doi:10.1007/s00216-014-7760-5, 2014.

Alves, C. A., Vicente, A. M., Custódio, D., Cerqueira, M., et al.: Polycyclic aromatic hydrocarbons and their derivatives (nitro-PAHs, oxygenated PAHs, and azaarenes) in $PM_{2.5}$ from Southern European cities, Science. of the Total. Environment. 595, 494–504, doi:10.1016/j.scitotenv.2017.03.256, 2017.

Abbas, I., Badran, G., Verdin, A., Ledoux, F., Roumie, M., Courcot, D.: Polycyclic aromatic hydrocarbon derivatives in airborne particulate matter: sources, analysis and toxicity, Environmental. Chemistry. Letters., 16, 439-475   doi.org/10.1007/s10311-017-0697-0, 2018.

Bezabeh, D.Z., Bamford, H.A., Schantz, M.M., Wise, S.A.: Determination of nitrated polycyclic aromatic hydrocarbons in diesel particulate-related standard reference materials by using gas chromatography/mass spectrometry with negative ion chemical ionization, Anal. Bioanal. Chem., 375, 381–388, doi:10.1007/s00216-002-1698-8, 2003.

Bamford, H. A. and Baker, J. E.: Nitro-polycyclic aromatic hydrocarbon concentrations and sources in urban and suburban atmospheres of the Mid-Atlantic region. Atmospheric. Environment., 37, 2077–2091. doi:10.1016/S1352-2310(03)00102-X, 2003.

Bond, T. C., Streets, D. G., Yarber, K. F., Nelson, S. M., Woo, J. H., Klimont, Z.: A technology-based global inventory of black and organic carbon emissions from combustion, J. Geophys. Res., 109, D14203, doi:10.1029/2003JD003697, 2004.

Bange, H.: Chapter 2 - Gaseous Nitrogen Compounds (NO, N_2O, N_2, NH_3) in the Ocean in Nitrogen in the Marine Environment (Second Edition), 51-94, 2008.

Bai, Z., Hu, Y., Yu, H., Wu, N., You, Y.: Quantitative health risk assessment of inhalation exposure to polycyclic aromatic hydrocarbons on citizens in Tianjin, China. Bull. Environ. Contam. Toxicol. 83, 151–154, doi: 10.1007/s00128-009-9686-8, 2009.

Benbrahim-Tallaa, L., Baan, R. A., Grosse, Y., Lauby-Secretan, B., El Ghissassi, F., Bouvard, V., et al.: Carcinogenicity of diesel-engine and gasoline-engine exhausts and some nitroarenes, Lancet. Oncol., 13, 663–664, doi:10.1016/S1470-2045(12)70280-2, 2012.

Bandowe, B.A.M., Meusel, H., Huang, R. J., Ho, K., Cao, J., Hoffmann, T., Wilcke, W.: $PM_{2.5}$-bound oxygenated PAHs, nitro-PAHs and parent-PAHs from the atmosphere of a Chinese megacity: Seasonal variation, sources and cancer risk assessment, Science. of the Total. Environment., 473–474, 77–87, doi: 10.1016/j.scitotenv.2013.11.108, 2014.

15

551 Ciccioli, P., Cecinato, A., Brancaleoni, E., Frattoni, M., Zacchei, P., Miguel, A.H.: Formation and transport of
552 2-nitrofluoranthene and 2-nitropyrene of photochemical origin in the troposphere, J. Geophys. Res., 101,
553 19567–19581, doi: 10.1029/95JD02118, 1996.

554 Chen, S.C. and Liao, C.M.: Health risk assessment on human exposed to environmental polycyclic aromatic
555 hydrocarbons pollution sources, Science. of the Total. Environment. 366, 112–123,
556 doi:10.1016/j.scitotenv.2005.08.047, 2006.

557 Chiang, H.L., Lai, Y.M., Chang, S.Y.: Pollutant constituents of exhaust emitted from light-duty diesel vehicles,
558 Atmospheric. Environment. 47, 399-406, doi:10.1016/j.atmosenv.2011.10.045, 2012.

559 Chen, Y., Li, X., Zhu, T., Han, Y., Lv, D.: PM2.5-bound PAHs in three indoor and one outdoor air in Beijing:
560 Concentration, source and health risk assessment, Science of the Total Environment 586, 255–264,
561 doi:10.1016/j.scitotenv.2017.01.214, 2017.

562 Durant, J.L., Busby Jr, W.F., Lafleur, A.L., Penman, B.W., Crespi, C.L.: Human cell mutagenicity of
563 oxygenated, nitrated and unsubstituted polycyclic aromatic hydrocarbons associated with urban aerosols, Mutat.
564 Res. Genet. Toxicol., 371, 123-157, doi:10.1016/S0165-1218(96)90103-2, 1996.

565 Dimashki, M., Harrad, S., Harrison, R.M.: Measurements of nitro-PAH in the atmospheres of two cities,
566 Atmospheric. Environment., 34, 2459-2469, doi:10.1016/S1352-2310(99)00417-3, 2000.

567 Feng, J., Chan, C. K., Fang, M., Hu, M., He, L., Tang, X.: Impact of meteorology and energy structure on
568 solvent extractable organic compounds of $PM_{2.5}$ in Beijing, China, Chemosphere. 61, 623–632,
569 doi:10.1016/j.chemosphere.2005.03.067, 2005.

570 Farren, N.J., Ramírez, N., Lee, J.D., Finessi, E., Lewis, A.C., Hamilton, J.F.: Estimated Exposure Risks from
571 Carcinogenic Nitrosamines in Urban Airborne Particulate Matter, Environ. Sci. Technol., 49, 9648−9656, doi:
572 10.1021/acs.est.5b01620, 2015.

573 Feng, B., Li, L., Xu, H., Wang, T., Wu, R., Chen, J., Zhang, Y., Liu, S., Ho, S.S.H., Cao, J., Huang, W.: $PM_{2.5}$-
574 bound polycyclic aromatic hydrocarbons (PAHs) in Beijing: Seasonal variations, sources, and risk assessment,
575 Journal. of Environmental. Sciences., 77, 11-19, doi:10.1016/j.jes.2017.12.025, 2019.

576 Goriaux, M., Jourdain, B., Temime, B., Besombes, J.-L., Marchand, N., Albinet, A., Leoz-Garziandia, E.
577 Wortham, H.: Field Comparison of Particulate PAH Measurements Using a Low-Flow Denuder Device and
578 Conventional Sampling Systems, Environ. Sci. Technol., 40, 6398–6404, doi:10.1021/es060544m, 2006.
579
580 Garrido-Frenich. A., Romero-González. R., Martínez-Vidal, J.L., Plaza-Bolaños. P., Cuadros-Rodríguez. L.,
581 Herrera-Abdo. M.A.: Characterization of recovery profiles using gas chromatography-triple quadrupole mass
582 spectrometry for the determination of pesticide residues in meat samples, Journal. of Chromatography. A., 1133,
583 315–321 doi:10.1016/j.chroma.2006.08.039, 2006.

584 Gao, Y., Ji, H.: Characteristics of polycyclic aromatic hydrocarbons components in fine particle during heavy
585 polluting phase of each season in urban Beijing, Chemosphere., 212, 346-357,
586 doi:10.1016/j.chemosphere.2018.08.079, 2018.

587   Hester, R.E., Harrison, R. M., Larsen J.C., Larsen P.B.: Air Pollution and Health, Chapter Chemical
588   carcinogens, Royal. Society. of Chemistry., 33–56, doi:10.1039/9781847550095, 1998.

589   Hannigan, M.P., Cass, G.R., Penman, B.W., Crespi, C.L., Lafleur, A.L., Busby, J. W., et al.: Bioassay-directed
590   chemical analysis of los angeles airborne particulate matter using a human cell mutagenicity assay, Environ. Sci.
591   Technol., 32, 3502–14, 1998.

592   Hamra, G. B., Guha, N., Cohen, A., Laden, F., et al.: Outdoor particulate matter exposure and lung cancer: a
593   systematic review and meta-analysis, Environ. Health. Perspect., 122, 906–911, doi:10.1289/ehp.1408092,
594   2014.

595   Janhäll, S., M. Jonsson, Å., Molnár, P., A. Svensson, E.; Hallquist, M.: Size resolved traffic emission factors of
596   submicrometer particles, Atmospheric. Environment., 38, 4331–4340, doi:10.1016/j.atmosenv.2004.04.018,
597   2004.

598   Jakober C.A., Riddle, S.G., Robert, M.A., Destaillats, H., Charles, M.J., Green, P.G., Kleeman, M.J.: Quinone
599   Emissions from Gasoline and Diesel Motor Vehicles, Environ. Sci. Technol., 41, 4548–54,
600   doi:10.1021/es062967u, 2007.

601   Jia, Y., Stone, D., Wang, W., Schrlau, J., Tao, S., Simonich, SL.: Estimated reduction in cancer risk due to PAH
602   exposures if source control measures during the 2008 Beijing Olympics were sustained, Environ. Health.
603   Perspect., 119, 815–20, 2011.

604   Jariyasopit, N., McIntosh, M., Zimmermann, K., Arey, J., Atkinson, R., et al.: Novel Nitro-PAH Formation
605   from Heterogeneous Reactions of PAHs with NO_2, NO_3/N_2O_5, and OH Radicals: Prediction, Laboratory
606   Studies, and Mutagenicity, Environ. Sci. Technol., 48, 412–419, doi:10.1021/es4043808, 2014.

607   Kawanaka, Y., Sakamoto, K., Wang, N., Yun, S-J.: Simple and sensitive method for determination of nitrated
608   polycyclic aromatic hydrocarbons in diesel exhaust particles by gas chromatography-negative ion chemical
609   ionisation tandem mass spectrometry, Journal. of Chromatography. A., 1163, 312–317,
610   doi:10.1016/j.chroma.2007.06.038, 2007.
611

612   Kim, K. H., Jahan, S. A., Kabir, E., Brown, R. J. C.: A review of airborne polycyclic aromatic hydrocarbons
613   (PAHs) and their human health effects, Environment International., 60, 71–80,
614   doi:10.1016/j.envint.2013.07.019, 2013.

615   Keyte, I. J., Harrison, R. M., Lammel, G.: Chemical reactivity and long-range transport potential of polycyclic
616   aromatic hydrocarbons – a review, Chem. Soc. Rev., 42, 9333 – 9391, doi:10.1039/C3CS60147A, 2013.

617   Keyte, I.J., Albinet, A., Harrison, R.M.: On-road traffic emissions of polycyclic aromatic hydrocarbons and their
618   oxy- and nitro- derivative compounds measured in road tunnel environments, Sci. Total. Environ., 566–567
619   1131-1142, doi:10.1016/j.scitotenv.2016.05.152, 2016.
620

621 Liu, Y., Tao, S., Yang, Y., Dou, H., Yang, Y., Coveney, R.M.: Inhalation exposure of traffic police officers to
622 polycyclic aromatic hydrocarbons (PAHs) during the winter in Beijing, China, Science. of the Total.
623 Environment., 383, 98 –105, doi:10.1016/j.scitotenv.2007.05.008, 2007.

624 Lee, C., Martin, Randal., Donkelaar, A. V., Lee, H., et al.: SO_2 emissions and lifetimes: Estimates from inverse
625 modeling using in situ and global, space-based (SCIAMACHY and OMI) observations, J. Geophys. Res., 116,
626 D06304, doi:10.1029/2010JD014758, 2011.

627 Liu, J., Man, R., Ma, S., Li, J., Wu, Q., Peng, J.: Atmospheric levels and health risk of polycyclic aromatic
628 hydrocarbons (PAHs) bound to $PM_{2.5}$ in Guangzhou, China, Marine. Pollution. Bulletin. 100, 134-143,
629 doi:10.1016/j.marpolbul.2015.09.014, 2015.

630 Liu, F., Beirle, S., Zhang, Q., Dörner, S., He, K., Wagner, T.: NOx lifetimes and emissions of cities and power
631 plants in polluted background estimated by satellite observations, Atmos. Chem. Phys., 16, 5283–5298,
632 doi:10.5194/acp-16-5283-2016, 2016.

633 Lin, Y., Zou, J., Yang, W., Li, C.Q.: A Review of Recent Advances in Research on $PM_{2.5}$ in China, Int. J.
634 Environ. Res. Public. Health., 15, 438, doi:10.3390/ijerph15030438, 2018.

635 Marr, L.C., Grogan, L.A., Wöhrnschimmel, H., Molina, L.T., Molina, M.J.: Vehicle Traffic as a Source of
636 Particulate Polycyclic Aromatic Hydrocarbon Exposure in the Mexico City Metropolitan Area, Environ. Sci.
637 Technol., 38, 2584–2592, doi:10.1021/es034962s, 2004.

638 Ministry of Ecology and Environment The People's Republic of China: Ambient air quality standards (GB-
639 3095-2012),
640 http://english.mee.gov.cn/Resources/standards/Air_Environment/quality_standard1/201605/t20160511_337502.
641 shtml

642 Ministry of Ecology and Environment The People's Republic of China: Beijing toughens pollution rules for
643 cleaner air (September 2013).
644 http://english.mee.gov.cn/News_service/media_news/201309/t20130903_259454.shtml
645 http://www.gov.cn/zwgk/2013-09-12/content_2486773.htm
646
647 Nisbet, I.C.T., LaGoy, P.K.: Toxic equivalency factors (TEFs) for polycyclic aromatic hydrocarbons (PAHs),
648 Regul. Toxicol. Pharmacol., 16, 290–300, doi:10.1016/0273-2300(92)90009-X, 1992.

649 Nalin, F., Golly, B., Besombes, J. L., Pelletier, C., Aujay-Plouzeau, R., Verlhac, S., Dermigny, A., Fievet, A.,
650 Karoski, N., Dubois, P., Collet, S., Favez, O., Albinet, A.: Fast oxidation processes from emission to ambient air
651 introduction of aerosol emitted by residential log wood stoves, Atmospheric Environment, 143, 15–26,
652 doi:10.1016/j.atmosenv.2016.08.002, 2016.
653
654 Nyiri, Z., Novák, M., Bodai, Z., Szabó, B. S., Ekea, Z., Zárayc, G., Szigeti, T.: Determination of particulate
655 phase polycyclic aromatic hydrocarbons and their nitrated and oxygenated derivatives using gas

chromatography–mass spectrometry and liquid chromatography–tandem mass spectrometry, Journal. of Chromatography. A., 1472, 88–98, doi: 10.1016/j.chroma.2016.10.021, 2016.

Niu, X., Ho, S. S. H., Ho, K. F., Huang, Y., Sun, J., Wang, Q., et al.: Atmospheric levels and cytotoxicity of polycyclic aromatic hydrocarbons and oxygenated-PAHs in PM$_{2.5}$ in the Beijing-Tianjin-Hebei region, Environmental. Pollution., 231, 1075-1084, doi: 10.1016/j.envpol.2017.08.099, 2017.

Office of Environmental Health Hazard Assessment (OEHHA).: Benzo[a]pyrene as a Toxic Air Contaminant. Available from: https://oehha.ca.gov/media/downloads/air/document/benzo5ba5dpyrene.pdf, 1994.

Office of Environmental Health Hazard Assessment (OEHHA).: Air Toxics Hot Spots Program Risk Assessment Guidelines. Part II: Technical Support Document for Describing Available Cancer Potency Factors. Office of Environmental Health Hazard Assessment. https://oehha.ca.gov/media/downloads/crnr/tsdnov2002.pdf, 105-109, 2002.

Office of Environmental Health Hazard Assessment (OEHHA).: Air Toxics Hot Spots Program Risk Assessment Guidelines. Part II: Technical Support Document for Describing Available Cancer Potency Factors. Office of Environmental Health Hazard Assessment. https://oehha.ca.gov/media/downloads/crnr/may2005hotspots.pdf, (8 and A1), 2005.

Purohit, V., Basu, A. K.: Mutagenicity of Nitroaromatic Compounds, Chem. Res. Toxicol., 13, 673−692, 2000.

Pio, C.A., Alves, C.A., Duarte, A.C.: Identification, abundance and origin of atmospheric organic particulate matter in a Portuguese rural area, Atmos. Environ., 35, 1365−1375, https://doi.org/10.1016/S1352-2310(00)00391-5, 2001.

Peng, L., Zhao, C., Lin, Y., Zheng, X., Tie, X., Chan, L. Y.: Analysis of carbon monoxide budget in North China, Chemosphere., 66, 1383−1389, doi:10.1016/j.chemosphere.2006.09.055, 2007.

Poulain, L., Iinuma, Y., Müller, K., Birmili, W., et al.: Diurnal variations of ambient particulate wood burning emissions and their contribution to the concentration of Polycyclic Aromatic Hydrocarbons (PAHs) in Seiffen, Germany, Atmos. Chem. Phys., 11, 12697-12713, doi:10.5194/acp-11-12697-2011, 2011.

Pietrogrande, M. C., Abbaszade, G., Schnelle-Kreis, J., Bacco, D., Mercuriali, M., Zimmermann, R.: Seasonal variation and source estimation of organic compounds in urban aerosol of Augsburg, Germany, Environmental. Pollution., 159, 1861-1868, doi:10.1016/j.envpol.2011.03.023, 2011.

Ramdahl, T., Zielinska, B., Arey, J., Atkinson, R., Winer, A. M., Pitts Jr, J. N.: Ubiquitous occurrence of 2-nitrofluoranthene and 2-nitropyrene in air, Nature., 321, 425-427, 1986.

Rogge, W.F., Hildemann, L.M., Mazurek, M.A., Cass, G.R., Simoneit, B.R.T.: Sources of fine organic aerosol. 2. Noncatalyst and catalyst-equipped automobiles and heavy-duty diesel trucks, Environ. Sci. Technol., 27, 636-651, doi:10.1021/es00041a007, 1993.

690

691 Reisen, F. and Arey, J.: Atmospheric reactions influence seasonal PAH and nitro-PAH concentrations in the Los

692 Angeles basin, Environ. Sci. Technol., 39, 64–73, doi:10.1021/es035454l, 2004.

693

694 Ravindra, K., Sokhi, R., Van Grieken, R.: Atmospheric polycyclic aromatic hydrocarbons: Source attribution,

695 emission factors and regulation, Atmospheric. Environment., 42, 2895–2921,

696 doi:10.1016/j.atmosenv.2007.12.010, 2008.

697

698 Ramírez, N., Cuadras, A., Rovira, Enric., Marcé, R.M., Borrull, F.: Risk Assessment Related to Atmospheric

699 Polycyclic Aromatic Hydrocarbons in Gas and Particle Phases near Industrial Sites, Environmental. Health.

700 Perspectives., 119, doi:10.1289/ehp.1002855, 2011.

701 Ringuet, J., Albinet, A., Leoz-Garziandia, E., Budzinski, H. and Villenave, E.: Reactivity of polycyclic aromatic

702 compounds (PAHs, NPAHs and OPAHs) adsorbed on natural aerosol particles exposed to atmospheric oxidants,

703 Atmospheric. Environment., 61, 15–22, doi:10.1016/j.atmosenv.2012.07.025, 2012a.

704

705 Ringuet, J., Albinet, A., Leoz-Garziandia, E., Budzinski, H., Villenave, E.: Diurnal/nocturnal concentrations and

706 sources of particulate-bound PAHs, OPAHs and NPAHs at traffic and suburban sites in the region of Paris

707 (France), Science. of the Total. Environment., 437, 297–305, doi.org/10.1016/j.scitotenv.2012.07.072, 2012b.

708 Raaschou-Nielsen, O., Andersen, N.Z., Beelen, R., et al.: Air pollution and lung cancer incidence in 17

709 European cohorts: prospective analyses from the European Study of Cohorts for Air Pollution Effects

710 (ESCAPE), Lancet. Oncol., 14, 813–822, doi: 10.1016/S1470-2045(13)70279-1, 2013.

711 Riva, M., Healy, R.M., Flaud, P.M., Perraudin, E., Wenger, J.C., Villenave, E.: Gas- and Particle-Phase

712 Products from the Chlorine-Initiated Oxidation of Polycyclic Aromatic Hydrocarbons, J. Phys. Chem. A., 119,

713 11170-11181, doi:10.1021/acs.jpca.5b04610, 2015.

714 Ramírez, N., Vallecillos, L., Lewis, A.C., Borrull, F., Marcé, R. M., Hamilton, J. F.: Comparative study of

715 comprehensive gas chromatography-nitrogen chemiluminescence detection and gas chromatography-ion trap-

716 tandem mass spectrometry for determining nicotine and carcinogen organic nitrogen compounds in thirdhand

717 tobacco smoke, Journal. of Chromatography. A., 1426, 191–200, doi:10.1016/j.chroma.2015.11.035, 2015.

718 Sasaki, J., Aschmann, SM., Kwok, E.S.C., Atkinson, R., Arey, J.: Products of the gas-phase OH and NO_3

719 radical-initiated reactions of naphthalene, Environ. Sci. Technol., 31, 3173–9, 1997.

720 Schauer, C., Neissner, R., Pöschl, U.: Polycyclic Aromatic Hydrocarbons in Urban Air Particulate Matter:

721 Decadal and Seasonal Trends, Chemical Degradation, and Sampling Artifacts., 37, 2861-2868,

722 doi:10.1021/es034059s, 2003.

723 Sharma, H., Jain, V.K., Khan, Z.H.: Characterization and source identification of polycyclic aromatic

724 hydrocarbons (PAHs) in the urban environment of Delhi, Chemosphere., 66, 302–310,

725 doi:10.1016/j.chemosphere.2006.05.003, 2007.

726 Saikawa, E., Naik, V., Horowitz, L. W., Liu, J. F., Mauzerall, D. L.: Present and potential future contributions of

727 sulfate, black and organic carbon aerosols from China to global air quality, premature mortality and radiative

728 forcing, Atmos. Environ., 43, 2814–2822, doi:10.1016/j.atmosenv.2009.02.017, 2009.

729 Shen, G., Tao, S., Wei, S., Zhang, Y., Wang, R., Wang, B., et al.: Emissions of parent, nitro, and oxygenated

730 polycyclic aromatic hydrocarbons from residential wood combustion in rural China, Environ. Sci. Technol., 46,

731 8123–30, doi:10.1021/es301146v, 2012.

732 Schulte, J.K., Fox, J.R., Oron, A.P., Larson, T.V., Simpson, C.D., Paulsen, M., Beaudet, N., Kaufman, J.D.,

733 Magzamen, S.: Neighborhood-scale spatial models of diesel exhaust concentration profile using 1-nitropyrene

734 and other nitroarenes, Environ. Sci. Technol., 49, 13422-13430, doi: 10.1021/acs.est.5b03639, 2015.

735

736 Srivastava, D., Favez, O., Bonnaire, N., Lucarelli, F., Haeffelin, M., Perraudin, E., Gros, V., Villenave, E.,

737 Albinet, A.: Speciation of organic fractions does matter for aerosol source apportionment. Part 2: Intensive

738 short-term campaign in the Paris area (France), Science. of The Total. Environment., 634, 267–278,

739 doi:10.1016/j.scitotenv.2018.03.296, 2018.

740

741 Song, H., Zhang, Y., Luo, M., Gu, J., Wu, M., Xu, D., Xu, G., Ma, L.: Seasonal variation, sources and health

742 risk assessment of polycyclic aromatic hydrocarbons in different particle fractions of $PM_{2.5}$ in Beijing, China,

743 Atmospheric Pollution Research., 10, 105-114, doi:10.1016/j.apr.2018.06.012, 2019.

744 Tsapakis, M. and Stephanou, E. G. Collection of gas and particle semi-volatile organic compounds: use of an

745 oxidant denuder to minimize polycyclic aromatic hydrocarbons degradation during high-volume air sampling,

746 Atmos. Environ., 37, 4935–4944, doi:10.1016/j.atmosenv.2003.08.026, 2003.

747 Tsapakis, M., and Stephanou, E. G: Diurnal Cycle of PAHs, Nitro-PAHs, and oxy-PAHs in a High Oxidation

748 Capacity Marine Background Atmosphere, Environ. Sci. Technol., 41, 8011–8017, doi: 10.1021/es071160e,

749 2007.

750 Tobiszewski, M., Namieśnik, J.: PAH diagnostic ratios for the identification of pollution emission sources,

751 Environmental. Pollution., 162, 110-119, doi:10.1016/j.envpol.2011.10.025, 2012.

752 Tomaz, S., Shahpoury, P., Jaffrezo, J.-L., Lammel, G., Perraudin, E., Villenave, E., Albinet, A.: One-year study

753 of polycyclic aromatic compounds at an urban site in Grenoble (France): Seasonal variations, gas/particle

754 partitioning and cancer risk estimation, Science. of The Total. Environment., 565, 1071–1083,

755 doi:10.1016/j.scitotenv.2016.05.137, 2016.

756

757 Tomaz, S., Jaffrezo, J.-L., Favez, O., Perraudin, E., Villenave, E., Albinet, A.: Sources and atmospheric

758 chemistry of oxy- and nitro-PAHs in the ambient air of Grenoble (France), Atmospheric. Environment., 161,

759 144–154, doi:10.1016/j.atmosenv.2017.04.042, 2017.

760 Tian,Y., Xiao,Z., Wang, H., et al.: Influence of the sampling period and time resolution on the PM source

761 apportionment: Study based on the high time-resolution data and long-term daily data, Atmos. Environ., 165,

762 301-309, doi:10.1016/j.atmosenv.2017.07.003, 2017.

763 World Health Organization (WHO), Air Quality Guidelines for Europe. 2nd ed. Copenhagen: WHO, Regional
764 Office for Europe (Copenhagen). http://www.euro.who.int/__data/assets/pdf_file/0005/74732/E71922.pdf,
765 Chapter 5, 92 – 94, 2000.

766 Wang, G., Kawamura, K., Lee, S., Ho, K., Cao, J.: Molecular, Seasonal, and Spatial Distributions of Organic
767 Aerosols from Fourteen Chinese Cities, Environ. Sci. Technol., 40, 4619-4625, doi:10.1021/es060291x, 2006.

768 Wang, W., Jariyasopit, N., Schrlau, J., Jia, Y., Tao, S., Yu, T.W., et al.: Concentration and Photochemistry of
769 PAHs, NPAHs, and OPAHs and Toxicity of PM$_{2.5}$ during the Beijing Olympic Games, Environ. Sci. Technol.,
770 45, 6887–95, doi:10.1021/es201443z, 2011a.

771 Wang, W., Huang, M.J., Kang, Y., Wang, H.S., Leung, A.O.W., Cheung, K.C., Wong, M.H.: Polycyclic
772 aromatic hydrocarbons (PAHs) in urban surface dust of Guangzhou, China: Status, sources and human health
773 risk assessment, Science. of the Total. Environment., 409, 4519–4527, doi:10.1016/j.scitotenv.2011.07.030,
774 2011b.

775 Wang, W., Simonich, S.L.M., Wang, W., Giri, B., Zhao, J., Xue, M., Cao, J., Lu, X., Tao, S.: Atmospheric
776 polycyclic aromatic hydrocarbon concentrations and gas/particle partitioning at background, rural village and
777 urban sites in the North China Plain, Atmospheric. Research., 99, 197–206, doi:10.1016/j.atmosres.2010.10.002,
778 2011c.

779 Wu, Y., Yang, L., Zheng, X., Zhang, S., Song, S., Li, J., Hao, J.: Characterization and source apportionment of
780 particulate PAHs in the roadside environment in Beijing, Science of the Total Environment 470-471, 76-83, doi:
781 10.1016/j.scitotenv.2013.09.066, 2014.

782 Wenyuan, Chen., and Tong Zhu.: Formation of Nitroanthracene and Anthraquinone from the Heterogeneous
783 Reaction Between NO$_2$ and Anthracene Adsorbed on NaCl Particles, Environ. Sci. Technol., 48, 8671–8678,
784 doi:10.1021/es501543g, 2014.

785 Wei, C., Bandowe, B.A.M., Han Y., Cao, J., Zhan, C., Wilcke, W.: Polycyclic aromatic hydrocarbons (PAHs)
786 and their derivatives (alkyl-PAHs, oxygenated-PAHs, nitrated-PAHs and azaarenes) in urban road dusts from
787 Xi'an, Central China, Chemosphere., 134, 512-520, doi:10.1016/j.chemosphere.2014.11.052, 2015.

788 World Health Organization (WHO), outdoor air pollution, IARC Monographs on the Evaluation of
789 Carcinogenic Risks to Humans, International Agency for Research on Cancer., 109, 2016.

790 Xu, S.S., Liu, W.X., Tao, S.: Emission of polycyclic aromatic hydrocarbons in China, Environ. Sci. Technol.,
791 40, 702–708, doi:10.1021/es0517062, 2006.

792 Yunker, M.B., Macdonald, R.W., Vingarzanc, R., Mitchell, R.H., Goyette, D., Sylvestre, S.: PAHs in the Fraser
793 River basin: a critical appraisal of PAH ratios as indicators of PAH source and composition, Org. Geochem., 33,
794 489–515, doi:10.1016/S0146-6380(02)00002-5, 2002.

795 Zhang, Y. X., Tao, S.: Global atmospheric emission inventory of polycyclic aromatic hydrocarbons (PAHs) for
796 2004, Atmos. Environ., 43, 812–819, doi:10.1016/j.atmosenv.2008.10.050, 2009.

797   Zimmermann, K., Jariyasopit, N., Massey Simonich, S. L., Tao, S., Atkinson, R., Arey, J.: Formation of Nitro-

798   PAHs from the Heterogeneous Reaction of Ambient Particle-Bound PAHs with $N_2O_5/NO_3/NO_2$, Environ. Sci.

799   Technol., 47, 8434−8442, doi:10.1021/es401789x, 2013.

800   Zhang, J., Yang, L., Mellouki, A., Chen, J., Chen, X., Gao, Y., Jiang, P., Li, Y., Yu, H., Wang, W.: Atmospheric

801   PAHs, NPAHs, and OPAHs at an urban, mountainous, and marine sites in Northern China: Molecular

802   composition, sources, and ageing, Atmos. Environ., 173, 256–264, doi:10.1016/j.atmosenv.2017.11.002, 2018.

803   Zhang, W., Tong, S., Ge, M., An, J., Shi, Z., Hou, S., Xia, K., Qu, Y., Zhang, H., Chu, B., Sun, Y., He, H.:

804   Variations and sources of nitrous acid (HONO) during a severe pollution episode in Beijing in winter 2016,

805   Science. of the Total. Environment., 648, 253–262, doi: 10.1016/j.scitotenv.2018.08.133, 2019.

806

807

808

809
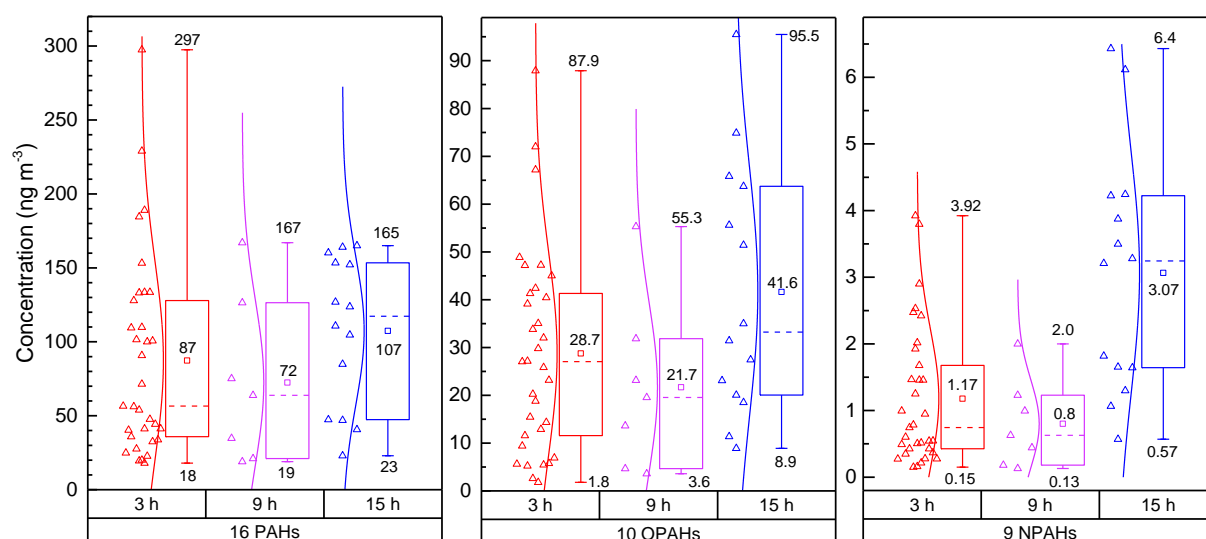
Figure 1. Concentrations of $\sum$PAHs, $\sum$OPAHs and $\sum$NPAHs in PM$_{2.5}$ samples during the daytime (3 h; 9 h) and night-time (15 h). Box plot represents the 25th and 75th percentiles range of the observed concentrations and the bottom and top lines indicate minimum and maximum concentrations. Square symbols represent the mean concentration, and the short dash line within the boxes represent the median. Empty Triangles correspond to the data measured over 3 h, 9 h and 15 h samples. The lines between data points and boxes reflect a normal distribution curve.

816

817

**Table 1. List of measured PAHs, OPAHs and NPAHs and their Abbreviations. Compounds are listed in order of elution.**

Compound/Formula	Abbreviation	Accurate Mass (m/z)	%RSD	
			Inter-day	Intra-day
16 PAHs		Monitored ions in EI mode		
Naphthalene/$C_{10}H_8$	NAP	128.0628-127.0543-102.0464	4.6	3.2
Acenaphthylene/$C_{12}H_8$	ACY	152.0629-151.0546-126.0463	4.1	2.1
Acenaphthene/ $C_{12}H_{10}$	AC	153.0705-154.0779-152.0634	5.5	6.1

Compound/Formula	Abbrev.	Monitored ions		
Fluorene/ $C_{13}H_{10}$	FLU	166.0782-165.0708-164.0621	4.0	2.9
Phenanthrene/$C_{14}H_{10}$	PHE	178.0789-176.0626-152.0622	4.6	3.0
Anthracene/$C_{14}H_{10}$	ANT	178.0787-176.0627-152.0620	4.7	4.2
Fluoranthene/$C_{16}H_{10}$	FLT	202.0788-200.0626-101.0388	1.8	4.5
Pyrene/$C_{16}H_{10}$	PYR	202.0788-200.0626-101.0389	3.2	1.9
Benzo[a]anthracene/$C_{18}H_{12}$	BaA	228.0927-226.0783-101.0388	6.2	1.2
Chrysene/$C_{18}H_{12}$	CHR	228.0943-226.0784-101.0387	6.0	2.6
Benzo[b]fluoranthene/$C_{20}H_{12}$	BbF	252.0941-250.0784-126.0467	4.7	2.0
Benzo[k]fluoranthene/$C_{20}H_{12}$	BkF	252.0940-250.0783-126.0468	8.9	8.7
Benzo[a]pyrene/$C_{20}H_{12}$	BaP	252.0940-250.0783-126.0466	5.2	2.3
Indeno[1,2,3-cd]pyrene/$C_{22}H_{12}$	IcdP	276.0939-274.0783-138.0467	7.2	2.6
Dibenz[a,h]anthracene/$C_{22}H_{14}$	DahA	278.1097-276.0941-139.0545	7.7	4.3
Benzo[ghi]perylene/$C_{22}H_{12}$	BghiP	276.0942-274.0783-138.0467	5.4	2.6
10 OPAHs		Monitored ions in NCI mode		
1,4-Naphtoquinone/$C_{10}H_6O_2$	1,4-NAQ	158.0420	6.3	5.1
1-Naphthaldehyde/$C_{11}H_8O$	1-NALD	156.0557	8.9	7.8
9-Fluorenone/$C_{13}H_8O$	9-FLON	180.0639	5.7	6.2
9,10-Anthraquinone/$C_{14}H_8O_2$	9,10-ANQ	208.0572	5.6	3.2
1,8-Naphthalic anhydride/ $C_{12}H_6O_3$	1,8-NANY	198.0436	6.4	5.6
Phenanthrene-9-carboxaldehyde/$C_{15}H_{10}O$	PHCA	206.0777	5.4	4.9
Benzo[a]fluorenone/ $C_{17}H_{10}O$	BaFLU	230.0791	6.4	3.2
7H-Benz[de]anthracene-7-one/ $C_{17}H_{10}O$	BANTone	230.0781	7.2	5.8
1-Pyrenecaboxaldehyde/ $C_{17}H_{10}O$	1-PYRCA	230.0786	7.5	7.2
1,2-Benzanthraquinone/ $C_{18}H_{10}O_2$	1,2-BANQ	258.0743	8.5	7.4
9 NPAHs		Monitored ions in NCI mode		
1-Nitronaphthalene/$C_{10}H_7NO_2$	1-NNAP	173.0551	4.7	4.4
3-Nitrodibenzofuran/ $C_{12}H_7NO_3$	3-NDBF	213.0475	4.4	5.1
5-Nitroacenaphthene/ $C_{12}H_9NO_2$	5-NAC	199.0682	5.6	5.3
2-Nitrofluorene/$C_{13}H_9NO_2$	2-NFLU	211.0689	5.0	5.4
9-Nitroanthracene/$C_{14}H_9NO_2$	9-NANT	223.0697	5.9	3.9
3-Nitrofluoranthene/$C_{16}H_9NO_2$	3-NFLT	247.0688	6.4	4.1
1-Nitropyrene/$C_{16}H_9NO_2$	1-NPYR	247.0691	3.9	3.2
6-Nitrochrysene/$C_{18}H_{11}NO_2$	6-NCHR	273.0847	4.7	5.4

6-Nitrobenzo[a]pyerene/ $C_{20}H_{11}NO_2$	6-NBaP	297.0845	8.4	9.7

820

821
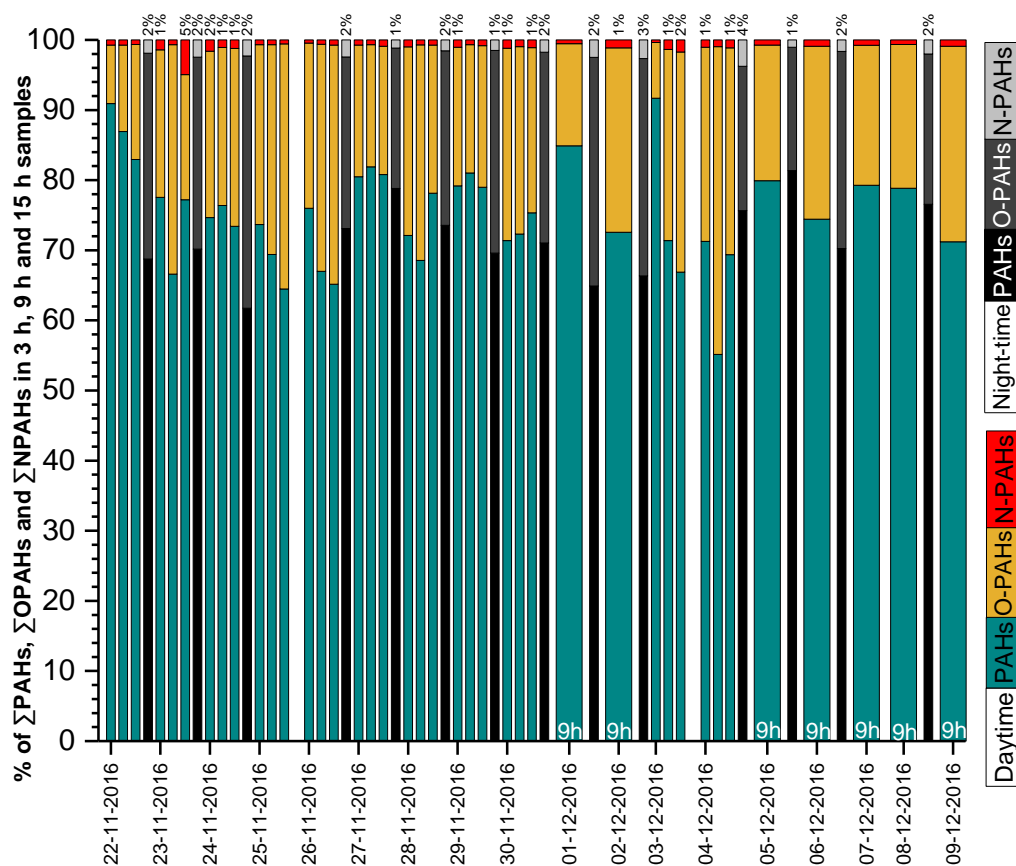
Figure 2. Time-series of ∑PAHs, ∑OPAHs and ∑NPAHs in PM$_{2.5}$ samples during the daytime (3 h and 9 h) and night-time (15h). Percentage below 1% for NPAHs are omitted for clarity. Night-time data on 25/11/2016, 03/12/2016 and 07/12/2016 are not available due to lack of samples.

822
823
824
825
826

827

828

829

830

Table 2. Minimum, maximum and average atmospheric concentrations of PAHs, OPAHs and NPAHs in PM$_{2.5}$.
Compounds in bold represent the highest mean contribution to the sum of all compounds.

Compound	Concentrations (ng m^{-3})		Average contribution
	Minimum-maximum	Average	to total (%)
16 PAHs	(3 h)/(9 h)/(15 h)	(3 h ± SD*)/(9 h ± SD)/(15 h ± SD)	(3 h)/(9 h)/(15 h)
NAP	(0.05-0.8)/(0.1-0.4)/(0.06-0.6)	(0.31 ± 0.2)/(0.24 ± 0.1)/(0.27 ± 0.2)	(0.48)/(0.39)/(0.25)
ACY	(0.01-1.2)/(0.1-0.8)/(0.1-1.2)	(0.31 ± 0.3)/(0.31 ± 0.2)/(0.58 ± 0.4)	(0.35)/(0.46)/(0.50)
AC	(0.03-0.13)/(0.02-0.09)/(0.01-0.2)	(0.07 ± 0.02)/(0.04 ± 0.03)/(0.07 ± 0.07)	(0.15)/(0.08)/(0.06)
FLU	(0.05-1.3)/(0.1-1.0)/(0.1-1.5)	(0.43 ± 0.3)/(0.41 ± 0.3)/(0.63 ± 0.4)	(0.53)/(0.65)/(0.56)
PHE	**(1.2-23.1)/(1.9-16.3)/(1.5-13.7)**	**(7.38 ± 5.5)/(6.30 ± 5.3)/(8.4 ± 4.0)**	**(8.83)/(9.04)/(7.84)**
ANT	(0.5-3.4)/(0.3-1.9)/(0.3-2.9)	(1.07 ± 0.7)/(0.79 ± 0.6)/(1.43 ± 0.8)	(1.48)/(1.23)/(1.32)
FLT	**(1.4-41.8)/(3.0-17.6)/(3.2-11.7)**	**(12.9 ± 10.0)/(9.10 ± 5.7)/(8.97 ± 2.7)**	**(13.9)/(13.9)/(9.67)**
PYR	**(0.7-34.6)/(2.1-15.7)/(2.9-10.7)**	**(9.85 ± 8.2)/(7.48 ± 5.0)/(8.1 ± 2.5)**	**(10.4)/(11)/(8.69)**
BaA	**(1.3-27.7)/(1.3-17.5)/(2.1-18.8)**	**(6.69 ± 6.4)/(6.52 ± 5.9)/(12 ± 5.9)**	**(7.17)/(8.23)/(11)**
CHR	**(1.4-37.5)/(2.1-20.8)/(2.7-15.9)**	**(10.5 ± 8.7)/(9.17 ± 7.17)/(11.3 ± 4.8)**	**(11.2)/(12.4)/(10.8)**
BbF	**(1.5-35.3)/(2.1-21.3)/(2.3-20.4)**	**(10.3 ± 8.5)/(8.93 ± 7.3)/(10.8 ± 5.0)**	**(11.2)/(11.8)/(10.4)**
BkF	(1.6-15.4)/(1.2-7.4)/(1.3-6.6)	(5.51 ± 3.8)/(3.94 ± 2.7)/(4.3 ± 1.5)	(6.76)/(5.80)/(4.43)
BaP	**(1.4-37.3)/(1.5-20.7)/(3.2-35.2)**	**(8.81 ± 8.6)/(8.40 ± 7.5)/(18.9 ± 12.4)**	**(9.12)/(10.3)/(16.1)**
IcdP	(1.7-16.1)/(0.9-11.6)/(1.0-18.3)	(4.79 ± 3.5)/(4.65 ± 4.3)/(9.75 ± 6.4)	(6.06)/(5.70)/(8.03)
DahA	(1.9-5.2)/(0.7-2.9)/(0.5-6.9)	(2.54 ± 0.7)/(1.46 ± 0.8)/(3.0 ± 2.1)	(4.43)/(2.46)/(2.56)
BghiP	(2.53-17.0)/(1.2-10.7)/(1.4-15.4)	(5.80 ± 3.5)/(4.70 ± 3.7)/(8.8 ± 5.1)	(7.86)/(6.47)/(7.62)
Total	(18-297)/(19-167)/(23-165)	(87.3 ± 58)/(72.5 ± 56)/(107 ± 51)	
10 OPAHs	(3 h)/(9 h)/(15 h)	(3 h ± SD)/(9 h ± SD)/(15 h ± SD)	(3 h)/(9 h)/(15 h)
1,4-NAQ	(0.02-8.1)/(0.16-3.1)/(0.1-4.2)	(2.25 ± 2.4)/(1.27 ± 1.2)/(1.66 ± 1.3)	(6.22)/(5.39)/(3.70)
1-NALD	(0.2-0.8)/(0.07-0.5)/(0.08-0.9)	(0.43 ± 0.1)/(0.20 ± 0.1)/(0.49 ± 0.3)	(2.71)/(1.19)/(1.25)
9-FLON	**(0.49-14.9)/(0.7-6.0)/(0.8-11.4)**	**(6.76 ± 4.4)/(2.56 ± 1.9)/(4.26 ± 2.8)**	**(25.8)/(14.3)/(10.2)**
9,10-ANQ	**(0.3-36.4)/(1.2-24.8)/(2.8-36)**	**(8.31 ± 8.8)/(8.65 ± 8.5)/(14.3 ± 9.9)**	**(24.3)/(35.8)/(32.7)**
1,8-NANY[a]	**(0.3-16.3)/(1.0-6.9)/(3.7-9.3)**	**(7.09 ± 5.4)/(3.69 ± 2.9)/(6.81 ± 2.8)**	**(37.9)/(33.2)/(45.6)**
PHCA	(0.1-0.9)/(0.05-0.6)/(0.06-1.9)	(0.26 ± 0.17)/(0.20 ± 0.19)/(0.71 ± 0.57)	(1.42)/(0.99)/(1.50)
BaFLU	(0.06-10.8)/(0.1-8.1)/(0.4-15.1)	(2.77 ± 3.0)/(2.72 ± 2.9)/(5.99 ± 4.8)	(7.47)/(9.73)/(12.1)
BANTone	(0.08-15.1)/(0.04-8.3)/(0.5-19.8)	(2.46 ± 3.3)/(2.63 ± 2.9)/(9.27 ± 7.3)	(6.10)/(9.05)/(19.1)
1-PYRCA	(0.007-1.8)/(0.008-1.5)/(0.05-2.4)	(0.31 ± 0.4)/(0.39 ± 0.5)/(1.0 ± 0.9)	(0.74)/(1.24)/(1.96)
1,2-BANQ	(0.02-3.6)/(0.03-2.6)/(0.2-3.9)	(0.87 ± 0.96)/(0.90 ± 0.96)/(1.99 ± 1.4)	(2.3)/(3.24)/(4.33)

26

Total	(1.8-87.9)/(3.6-55.3)(8.9-95.5)	(28.7 ± 21)/(21.7 ± 18)/(41.6 ± 26)	
9 NPAHs	(3 h)/(9 h)/(15 h)	(3 h ± SD)/(9 h ± SD)/(15 h ± SD)	(3 h)/(9 h)/(15 h)
1-NNAP	(0.01-0.1)/(0.008-0.04)/(0.005-0.03)	(0.03 ± 0.02)/(0.01 ± 0.01)/(0.01 ± 0.008)	(4.38)/(3.08)/(0.57)
3-NDBF	**(0.08-1.5)/(0.02-0.06)/(0.03-2.4)**	**(0.33 ± 0.31)/(0.03 ± 0.01)/(0.89 ± 0.84)**	**(33.4)/(7.92)/(22.4)**
5-NAC[b]	(0.04-0.1)/(<LOQ)/(0.03-0.35)	(0.08 ± 0.05)/(<LOQ)/(0.18 ± 0.13)	(5.64)/(<LOQ)/(4.67)
2-NFLU	(0.03-0.3)/(0.01-0.3)/(0.01-0.5)	(0.08 ± 0.06)/(0.09 ± 0.11)/(0.26 ± 0.21)	(10.15)/(10.00)/(7.28)
9-NANT	**(0.01-1.2)/(0.06-0.1)/(0.4-2.4)**	**(0.36 ± 0.37)/(0.41 ± 0.31)/(1.18 ± 0.6)**	**(27.1)/(53.4)/(47.5)**
3-NFLT	**(0.05-1.2)/(0.02-0.5)/(0.04-1.2)**	**(0.34 ± 0.3)/(0.21 ± 0.2)/(0.54 ± 0.4)**	**(24.6)/(23.4)/(17.7)**
1-NPYR[c]	(0.01-0.1)/(0.01-0.06)/(0.008-0.2)	(0.05 ± 0.03)/(0.06 ± 0.05)/(0.02 ± 0.02)	(2.92)/(2.48)/(2.01)
6-NCHR[d]	(0.05-0.2)/(<LOQ)/(0.009-0.02)	(0.09 ± 0.06)/(<LOQ)/(0.01 ± 0.007)	(5.6)/(<LOQ)/(0.5)
6-NBaP[e]	(<LOQ)/(<LOQ)/(0.02-0.08)	(<LOQ)/(<LOQ)/(0.05 ± 0.01)	(<LOQ)/(<LOQ)/(1.26)
Total	(0.15-3.92)/(0.13-2.0)/(0.57-6.43)	(1.17 ± 1.0)/(0.80 ± 0.66)/(3.06 ± 1.8)	

833   [a] Quantified in 28/54 samples
834   [b] Quantified in 7/54 samples
835   [c] Quantified in 35/54 samples
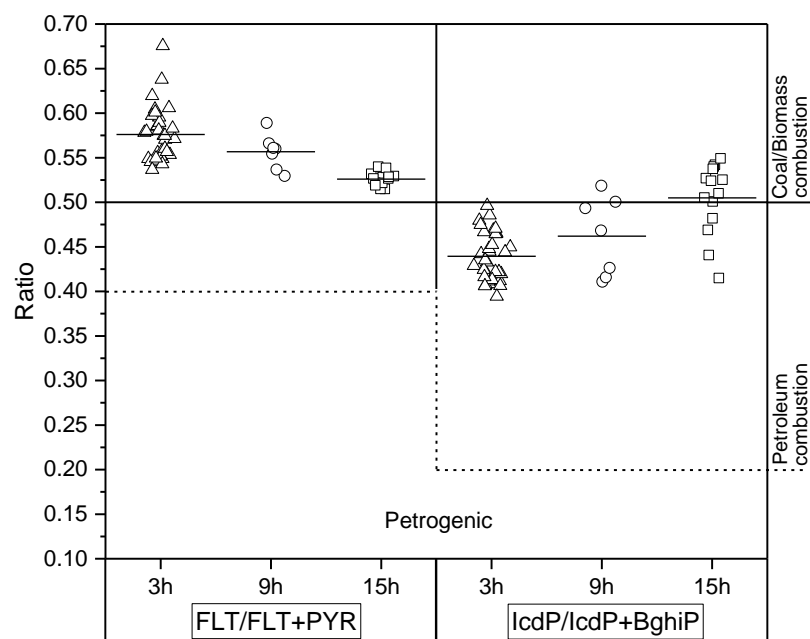836   [d] Quantified in 5/54 samples
837   [e] Quantified in 11/54 samples
838   * SD: Standard Deviation
839

840

841

842

843

Figure 3. Column scatter of FLT/(FLT + PYR) and IcdP/(IcdP + BghiP) in the particulate phase at three different time sampling averages, open triangles and circles represent the daytime data for 3 h and 9 h samples, open squares represent the night-time data of 15 h. The dashed line separates the petroleum combustion source from petrogenic source for both ratios. The solid short line on each data set represent the mean value of ratios.

848

849

850 **Table 3. Average concentration of $\sum BaP_{eq}$ in ng m^{-3} and cancer risk assessment for the sum of 16PAHs, 1OPAH and 6NPAHs.**

| Sampling hours	$\sum[BaP]_{eq}$ ng m^{-3}	$UR_{BaP} = 1.1 \times 10^{-6}$ (CalEPA)	$UR_{BaP} = 8.7 \times 10^{-5}$ (WHO)	Risk per million people
9 h (daytime, n=40)[a]	15.9[a]	1.75×10^{-5}	1.38×10^{-3}	17[b] – 1383[c]
15 h (night-time, n=14)	28.3	3.17×10^{-5}	2.46×10^{-3}	31[b] – 2460[c]
24 h (n=54)	**23.6**	**2.6×10^{-5}**	**2.05×10^{-3}**	**26[b] – 2053[c]**

852 [a] Average includes combined 3 h samples in each day (n=33) and 9 h samples (n=7)
853 [b] Calculated Value according to CalEPA
854 [c] Calculated Value according to WHO
855 n: number of samples
856

857
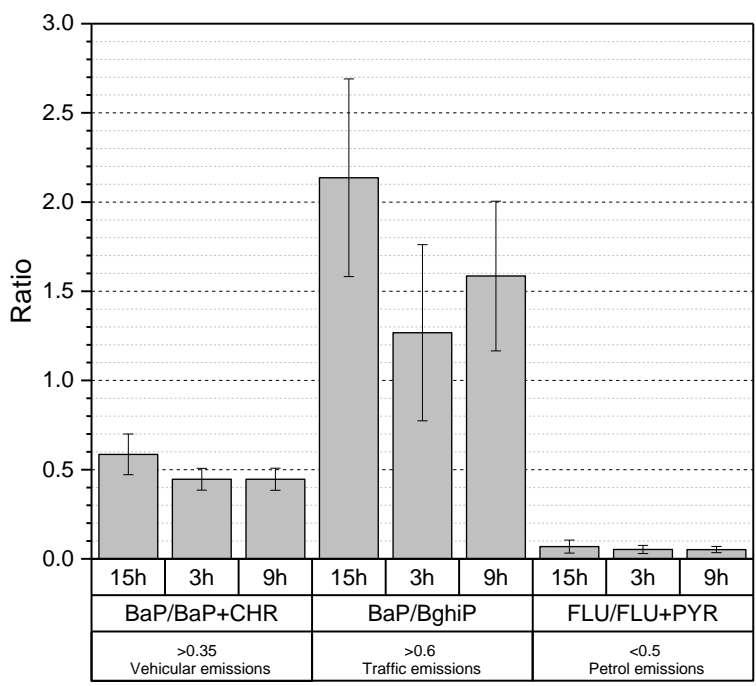
Figure 4. Column distribution of BaP/BaP+CHR, BaP/BghiP and FLU/FLU+PYR in the particulate phase for three different sampling periods. 3 h and 9 h represent samples collected during the day and 15 h for samples at night. Error bars reflect standard deviations.

861

862

863

864

865

866

867

868

869

870

871

872

873

874

875

876

877
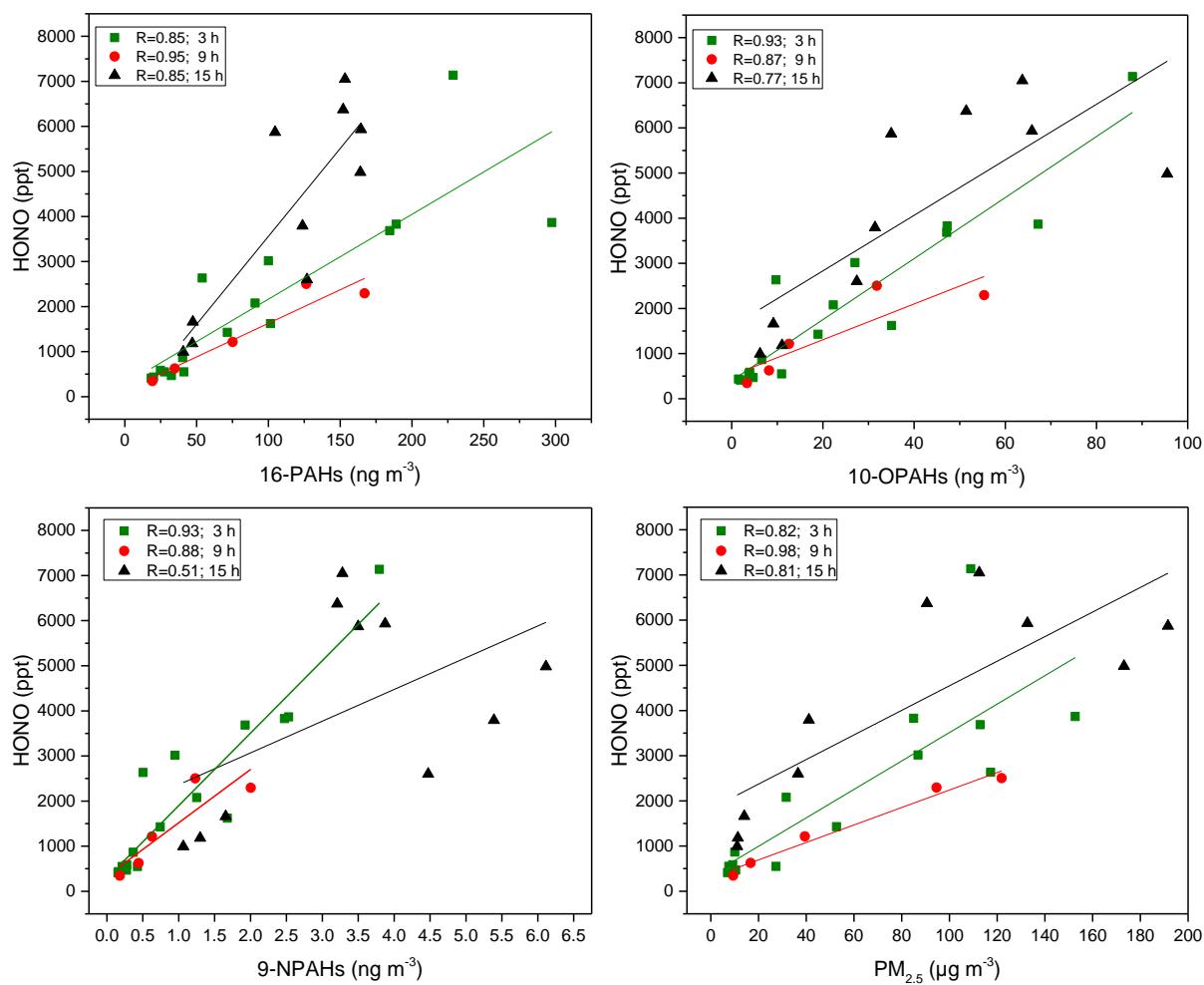
Figure 5. Correlation coefficients of ∑PAHs, ∑OPAHs, ∑NPAHs and PM₂.₅ with HONO. Time sampling resolution of 3 h and 9 h refer to daytime concentrations and 15 h to nocturnal concentrations. Significance levels were between 0.001 and 0.05 except for HONO and NPAHs at night, P level > 0.05 and Pearson coefficient 0.52.
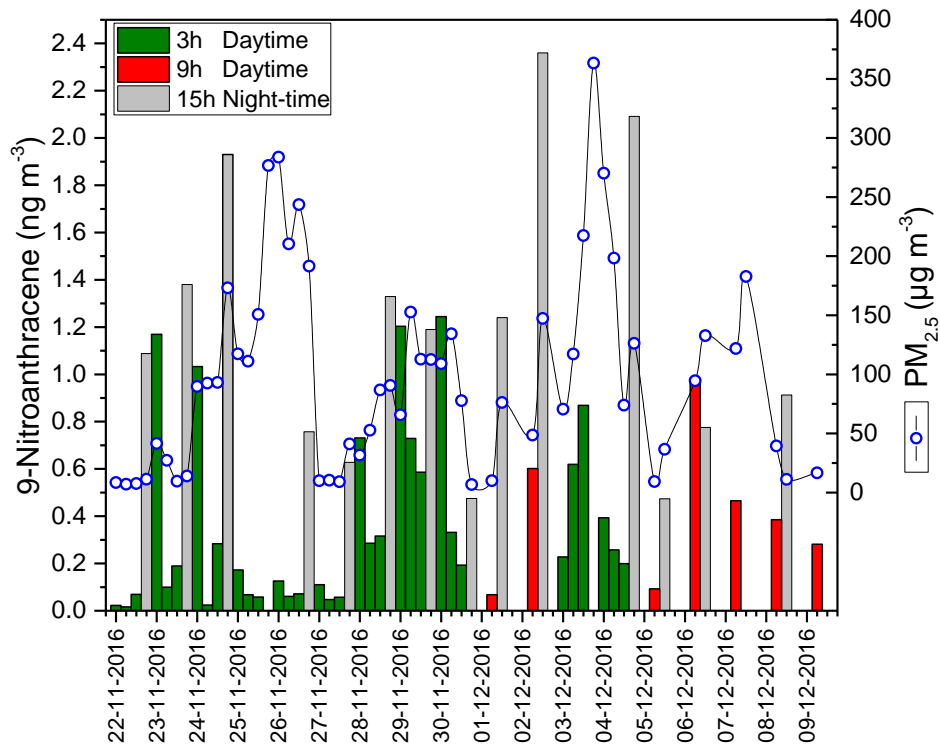
883

884

885 **Figure 6. Temporal variation of 9-Nitroanthrance and PM$_{2.5}$ over the entire winter campaign.**

886